ICP-1050-II

LMFBR - Fuel Recycle
TID-4500
UC-79c

FAST REACTOR FISSION YIELDS FOR ^{239}Pu and ^{241}Pu

Edited by
W. J. Maeck

ALLIED CHEMICAL CORPORATION
IDAHO CHEMICAL PROGRAMS - OPERATIONS OFFICE

Date Published - August 1977

Prepared for the
Energy Research & Development Administration
Under Contract No. EY-76-C-07-1540

ABSTRACT

Fast fission yield data are presented for ^{239}Pu and ^{241}Pu irradiated in EBR-II. The measurement technique was isotope dilution mass spectrometry. The neutron environment for the irradiation is defined, and chemical separation and mass spectrometric procedures are briefly described. Recommendations and suggestions for the selection of burnup monitors are given.

SUMMARY

In this report of a continuing program dedicated to the measurement of fast reactor fission yields and the selection of burnup monitors for fast breeder reactor (FBR) fuels, measured absolute fast reactor fission yields are presented for the stable and long-lived isotopes of Kr, Rb, Sr, Zr, Mo, Ru, Sb, Xe, Cs, Ba, La, Ce, Nd, and Sm for ^{239}Pu and ^{241}Pu irradiated in EBR-II. The principal measurement technique was isotope dilution mass spectrometry. Yield measurements for ^{233}U, ^{235}U, and ^{238}U have been previously reported in USERDA Rept. ICP-1050-I. In the future, these data will be augmented by fast fission yield data for ^{240}Pu, ^{242}Pu, ^{237}Np, and ^{241}Am. The results of extensive flux measurements to characterize the neutron spectrum associated with the irradiation are presented. For mixed oxide fuels where the major sources of fission are ^{235}U and ^{239}Pu and the neutron spectrum is characteristic of a mixed-oxide fueled LMFBR, the preferred monitor for the determination of burnup is ^{148}Nd and a fission yield of 1.66%.

CONTRIBUTING PERSONNEL

The wide scope of this project required contributions from a number of scientists and technicians with specialized disciplines. Listed below are individuals who provided significant contributions and made this report possible.

Chemistry

D. E. Adams
W. A. Emel
F. A. Duce
R. L. Eggleston
A. L. Erikson
J. H. Keller
R. L. Tromp

Mass Spectrometry

L. W. Buttars
J. E. Delmore
L. L. Dickerson
R. A. Nielsen

Statistics

J. W. Meteer
F. W. Spraktes

CONTENTS

ABSTRACT..... i

SUMMARY..... ii

I. INTRODUCTION..... 1

II. IRRADIATION PACKAGE..... 1

II-A. FISSION YIELD CAPSULES..... 3

II-B. NEUTRON SPECTRUM MONITOR CAPSULES..... 3

II-C. CAPTURE-TO-FISSION RATIO CAPSULES..... 3

III. SAMPLE DISSOLUTION AND ANALYSIS..... 5

III-A. FISSION YIELD SAMPLES..... 5

III-B. SPECTRUM MONITOR SAMPLES..... 7

III-C. CAPTURE-TO-FISSION RATIO SAMPLES..... 8

IV. DETERMINATION OF NUMBER OF FISSIONS..... 8

V. ^{239}Pu FAST FISSION YIELDS..... 9

V-A. ISOTOPIC COMPOSITION OF FISSION PRODUCT ELEMENTS..... 9

V-B. ABSOLUTE FISSION YIELDS..... 11

V-B-1. Heavy Mass Peak..... 12

V-B-1-a. Mass Region 119-124..... 12

V-B-1-b. Mass 125..... 12

V-B-1-c. Mass Region 126-130..... 12

V-B-1-d. Xenon (Mass 131, 132, 134, 136)..... 12

V-B-1-e. Cesium (Mass 133, 135, 137)..... 13

V-B-1-f. Barium (Mass 138)..... 14

V-B-1-g. Lanthanum (Mass 139)..... 15

V-B-1-h. Cerium (Mass 140, 142)..... 15

V-B-1-i. Mass 141..... 16

V-B-1-j. Neodymium (Mass 143, 144, 145, 146, 148, 150)..... 16

V-B-1-K. Samarium (Mass 147,149,151,152,154)... 18
V-B-1-ℓ. Mass 153..... 19
V-B-1-m. Mass Region 156 to 160..... 19
V-B-2. Light Mass Peak..... 19
V-B-2-a. Mass Region 75 to 82..... 19
V-B-2-b. Krypton (Mass 83, 84, 86)..... 19
V-B-2-c. Rubidium (Mass 85,87)..... 20
V-B-2-d. Strontium (Mass 88, 90)..... 21
V-B-2-e. Mass 89..... 21
V-B-2-f. Zirconium (Mass 91, 92, 93, 94, 96)... 21
V-B-2-g. Molybdenum (Mass 95, 97, 98, 100)..... 22
V-B-2-h. Mass 99..... 22
V-B-2-i. Ruthenium (Mass 101, 102, 103, 104, 105, 106)..... 23
V-B-2-j. Mass 107, 108, 109, 110..... 25
V-B-2-k. Mass 111..... 25
V-B-2-ℓ. Mass 112-118..... 26
V-C. ERROR ANALYSIS 26
VI. ^{241}Pu FAST FISSION YIELDS..... 33
VI-A. ISOTOPIC COMPOSITION OF FISSION PRODUCT ELEMENTS..... 33
VI-B. ABSOLUTE FISSION YIELDS..... 33
VI-B-1. Heavy Mass Peak..... 34
VI-B-1-a. Mass Region 120-124..... 34
VI-B-1-b. Mass 125..... 34
VI-B-1-c. Mass Region 126-130..... 34
VI-B-1-d. Xenon (Mass 131, 132, 134, 136).... 34
VI-B-1-e. Cesium (Mass 133, 135, 137)..... 34
VI-B-1-f. Barium (Mass 138)..... 36
VI-B-1-g. Lanthanum (Mass 139)..... 36
VI-B-1-h. Cerium (Mass 140, 142)..... 37

VI-B-1-i. Mass 141..... 37

VI-B-1-j. Neodymium (Mass 143, 144, 145, 146, 148, 150)..... 37

VI-B-1-k. Samarium (Mass 147, 149, 151, 152, 154)..... 39

VI-B-1-ℓ. Mass 153..... 40

VI-B-1-m. Mass Region 156-160..... 40

VI-B-2. Light Mass Peak..... 40

VI-B-2-a. Mass Region 75-82..... 40

VI-B-2-b. Krypton (Mass 83, 84, 86)..... 40

VI-B-2-c. Rubidium (Mass 85, 87)..... 41

VI-B-2-d. Strontium (Mass 88, 90)..... 42

VI-B-2-e. Mass 89..... 42

VI-B-2-f. Zirconium (Mass 91, 92, 93, 94, 96)..... 42

VI-B-2-g. Molybdenum (Mass 95, 97, 98, 100)..... 43

VI-B-2-h. Mass 99..... 43

VI-B-2-i. Ruthenium (Mass 101, 102, 103, 104, 105, 106)..... 44

VI-B-2-j. Mass Region 107-112..... 45

VI-B-2-ℓ. Mass 113-119..... 45

VI-C. ERROR ANALYSIS..... 45

VII. BURNUP MONITORS..... 50

REFERENCES..... 51

APPENDIX..... 52

A-1. Rubidium, Cesium, Strontium, and Barium..... 53

A-2. Lanthanum, Cerium, Neodymium, and Samarium..... 54

A-3. Zirconium..... 55

A-4. Molybdenum..... 56

A-5. Ruthenium..... 57

FIGURES

1. EBR-II Irradiation Assembly - Location of Fission Yield Spectrum Monitor, and Capture-to-Fission Ratio Capsules..... 4

2. Dissolution and Gas Collection Apparatus..... 6

TABLES

I. IRRADIATION AND NEUTRON SPECTRUM DATA..... 2

II. SPECTRUM MONITORS..... 3

III. COMPONENTS AND ERRORS RELATIVE TO DETERMINING THE NUMBER OF FISSIONS..... 10

IV. ISOTOPIC COMPOSITION OF XENON FROM ^{239}Pu FAST AND THERMAL FISSION..... 13

V. ISOTOPIC COMPOSITION OF CESIUM FROM ^{239}Pu FAST AND THERMAL FISSION..... 14

VI. ISOTOPIC COMPOSITION OF CERIUM FROM ^{239}Pu FAST AND THERMAL FISSION..... 15

VII. ISOTOPIC COMPOSITION OF NEODYMIUM FROM ^{239}Pu FAST AND THERMAL FISSION..... 17

VIII. ISOTOPIC COMPOSITION OF SAMARIUM FROM ^{239}Pu FAST AND THERMAL FISSION..... 18

IX. ISOTOPIC COMPOSITION OF KRYPTON FROM ^{239}Pu FAST AND THERMAL FISSION..... 20

X. ISOTOPIC COMPOSITION OF RUBIDIUM FROM ^{239}Pu FAST AND THERMAL FISSION..... 20

XI. ISOTOPIC COMPOSITION OF STRONTIUM FROM ^{239}Pu FAST AND THERMAL FISSION..... 21

XII. ISOTOPIC COMPOSITION OF ZIRCONIUM FROM ^{239}Pu FAST AND THERMAL FISSION..... 22

XIII. ISOTOPIC COMPOSITION OF MOLYBDENUM FROM ^{239}Pu FAST AND THERMAL FISSION..... 23

XIV. ISOTOPIC COMPOSITION OF RUTHENIUM FROM ^{239}Pu FAST AND THERMAL FISSION..... 24

XV. MEASURED ATOMS AND FAST FISSION YIELDS FOR ^{239}Pu - CAPSULE 5..... 27

XVI. MEASURED ATOMS AND FAST FISSION YIELDS FOR ^{239}Pu - CAPSULE 24 28

XVII. MEASURED ATOMS AND FAST FISSION YIELDS FOR ^{239}Pu - CAPSULE 26 29

XVIII. SUMMARY ^{239}Pu FAST FISSION YIELDS 30

XIX. MEASURED ATOMS AND FAST FISSION YIELDS FOR ^{239}Pu - CAPSULE 35 32

XX. ISOTOPIC COMPOSITION OF XENON FROM ^{241}Pu FAST AND THERMAL FISSION 35

XXI. ISOTOPIC COMPOSITION OF CESIUM FROM ^{241}Pu FAST AND THERMAL FISSION 36

XXII. ISOTOPIC COMPOSITION OF CERIUM FROM ^{241}Pu FAST AND THERMAL FISSION 37

XXIII. ISOTOPIC COMPOSITION OF NEODYMIUM FROM ^{241}Pu FAST AND THERMAL FISSION 38

XXIV. ISOTOPIC COMPOSITION OF SAMARIUM FROM ^{241}Pu FAST AND THERMAL FISSION 39

XXV. ISOTOPIC COMPOSITION OF KRYPTON FROM ^{241}Pu FAST AND THERMAL FISSION 41

XXVI. ISOTOPIC COMPOSITION OF RUBIDIUM FROM ^{241}Pu FAST AND THERMAL FISSION 41

XXVII. ISOTOPIC COMPOSITION OF STRONTIUM FROM ^{241}Pu FAST AND THERMAL FISSION 42

XXVIII. ISOTOPIC COMPOSITION OF ZIRCONIUM FROM ^{241}Pu FAST AND THERMAL FISSION 43

XXIX. ISOTOPIC COMPOSITION OF MOLYBDENUM FROM ^{241}Pu FAST AND THERMAL FISSION 44

XXX. ISOTOPIC COMPOSITION OF RUTHENIUM FROM ^{241}Pu FAST AND THERMAL FISSION 45

XXXI. MEASURED ATOMS AND FAST FISSION YIELDS FOR ^{241}Pu - CAPSULE 18 46

XXXII. MEASURED ATOMS AND FAST FISSION YIELDS FOR ^{241}Pu - CAPSULE 39 47

XXXIII. SUMMARY ^{241}Pu FAST FISSION YIELDS 48

I. INTRODUCTION

Based on a review[1] of the nuclear data and analytical chemistry methodology requirements for the accurate determination of burnup for fast reactor fuels, conducted in 1973, it was concluded that the preferred method for measuring burnup in a Fast Breeder Reactor (FBR) was the fission product-residual heavy atom method. Specifically noted, was that the largest source of error in this method was the uncertainty of the fission yield values used to establish the number of fissions. In 1973, the fast fission yields were limited to ^{235}U and ^{239}Pu which had been measured on samples irradiated in a neutron spectrum much harder than that expected for large commercial FBRs. Essentially, no reliable fast reactor fission yield data were available for the other heavy isotopes (ie, ^{238}U, ^{240}Pu, ^{241}Pu, ^{242}Pu) which could be sources of fission in FBR fuels, nor for ^{233}U which is used in experimental FBR fuel development studies.

Thus, a program is under way to accurately measure absolute fast reactor fission yields for many heavy element nuclides in a neutron spectrum characteristic of mixed oxide fueled LMFBRs, and to develop and proof test reliable methods for the accurate determination of burnup in a variety of fuels. Fast reactor fission yields for over 40 stable and long-lived isotopes from samples of ^{233}U, ^{235}U, and ^{238}U irradiated in the Experimental Breeder Reactor-II (EBR-II) were published in 1975.[2] Also reported at that time were preliminary fast fission yields for ^{239}Pu, based on the analysis of two samples irradiated in EBR-II.

This report gives fast reactor fission yield data obtained from four samples of ^{239}Pu and two samples of ^{241}Pu irradiated in EBR-II. The reported ^{239}Pu data supersedes that given in ICP-1050-I[2].

II. IRRADIATION PACKAGE

The sample irradiation was conducted in Row 8 of EBR-II. The irradiation package contained multiple capsules of ^{233}U, ^{235}U, ^{238}U, ^{237}Np, ^{239}Pu, ^{240}Pu, ^{241}Pu, ^{242}Pu, ^{241}Am, and ^{243}Am for fission yield measurements, spectrum monitors to characterize the neutron spectrum, and samples of ^{233}U, ^{235}U, ^{239}Pu, ^{240}Pu, ^{241}Pu, and ^{242}Pu for the

TABLE I

IRRADIATION AND NEUTRON SPECTRUM DATA

Reactor - Experimental Breeder Reactor II (EBR-II), Idaho National Engineering Laboratory (INEL), Idaho Falls, Idaho

Irradiation Time - 1340 h with reactor at 62.5 Mw. Down time while samples were in reactor - 1500 h.

Position - Row-8 (See Figure 1)

	^{239}Pu CAPSULES				^{241}Pu CAPSULES	
Capsule Number	5	24	26	35	18	39
Capsule content - mg PuO_2	755	659	754	771	638	755
^{238}Pu, atom %			---		<0.009	
^{239}Pu			99.100		0.862	
^{240}Pu			0.888		2.973	
^{241}Pu			0.014		94.636	
^{242}Pu			---		1.520	
Location, +cm above and -cm below midplane	+12cm	-7cm	+9cm	+38cm	+30cm	+38cm
Est. flux, $n/cm^2/s$	8.2E14	8.8E14	7.5E14	2.8E14	5.0E14	3.5E14
Mean neutron energy, keV	460	485	455	225	350	275
Mean fission energy, ^{239}Pu, keV	450	480	440	210	---	---
Mean fission energy, ^{241}Pu, keV	---	---	---	---	200	170
Spectral Index, $^{238}U/^{235}U$ Reaction rate	0.018	0.020	0.018	0.004	∿.007	0.004
$^{150}Nd/^{143}Nd$ Isotopic Ratio	0.2238	0.2247	0.2238	0.2215	0.2590	0.2587

measurement of the capture-to-fission ratio, α. Details relative to capsule contents, irradiation time, reactor location, estimated flux levels, and neutron spectrum are given in Table I.

II-A. FISSION YIELD CAPSULES

The highly enriched target isotopes as oxide powders were individually mixed with high purity (99.99+%) nickel powder, weld-sealed in nickel capsules machined from 99.99+% pure nickel rod, and loaded into a standard EBR-II, B-7A subassembly for the irradiation. The geometry of the sample loading and the location of the ^{239}Pu and ^{241}Pu samples are shown in Figure 1.

II-B. NEUTRON SPECTRUM MONITOR CAPSULES

To characterize the neutron spectrum, twelve spectrum monitor capsules, each containing nine monitors, were included in the irradiation package as shown in Figure 1. Table II lists the monitors, the nuclear reactions, and the measured reaction products.

II-C. CAPTURE-TO-FISSION RATIO CAPSULES

For the determination of α, three nickel capsules, each containing duplicate oxide samples of highly enriched ^{233}U, ^{235}U, ^{239}Pu, ^{240}Pu, ^{241}Pu, and ^{242}Pu sealed in stainless steel needles were irradiated. These capsules were located adjacent to the spectrum monitor capsules as shown in Figure 1.

TABLE II

SPECTRUM MONITORS

Monitor	Reaction	Measured Product
Co wire	n,γ	^{60}Co
Sc powder	n,γ	^{46}Sc
Fe wire	n,p	^{54}Mn
Ni wire	n,p	^{58}Co
Ti wire	n,p	^{46}Sc
Cu wire	n,α	^{60}Co
^{237}Np oxide	n,f	^{137}Cs
^{238}U oxide	n,f	^{137}Cs
^{235}U oxide	n,f	^{137}Cs

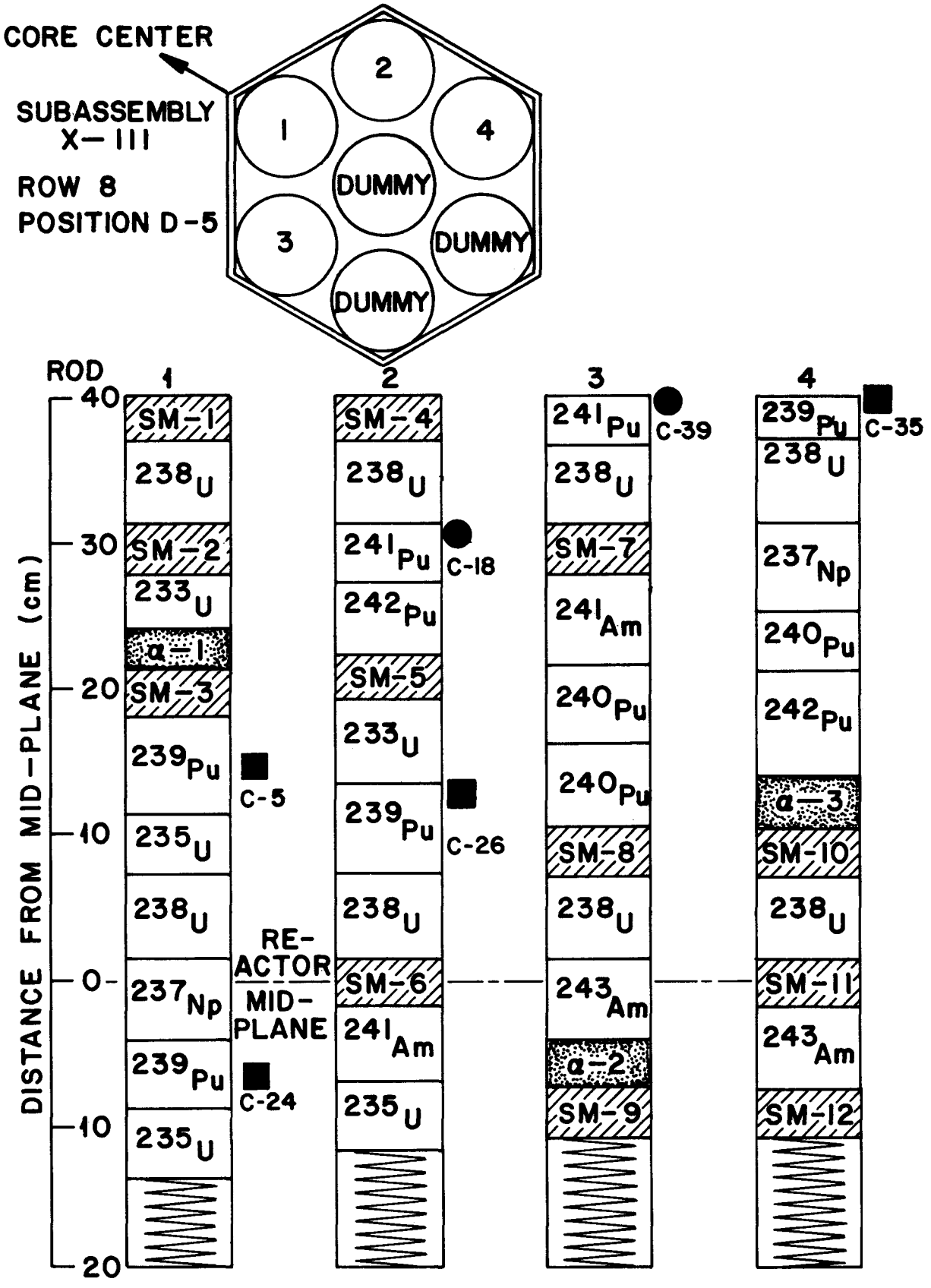

Fig. 1 EBR-II Irradiation Assembly - Location of Fission Yield Spectrum Monitor, and Capture-to-Fission Ratio Capsules.

III. SAMPLE DISSOLUTION AND ANALYSIS

III-A. FISSION YIELD SAMPLES

The ^{239}Pu and ^{241}Pu samples were dissolved using a mixture of 8M HNO_3-0.1M HF in a quartz flask equipped with a quartz reflux condenser. A schematic diagram of the dissolution and gas collection apparatus is shown in Figure 2. Initially, the sample to be dissolved was placed in the quartz dissolver containing 50 ml of quartz-distilled water, and the entire system was purged with He. After purging, a slight positive pressure was placed on the system and all joints were monitored with a He leak detector to establish system integrity. The dissolving acid was added in 100-ml increments and the temperature of the dissolver was increased. When the clad had been violated as evidenced by the detection of ^{85}Kr activity, measured quantities of $^{78-80}Kr$ and ^{129}Xe isotopic spikes were introduced into the dissolution flask from the spike-addition manifold by switching the helium flow. The inert gases were swept from the dissolver flask and through the collection train (Figure 2) with helium at a flow of ~100 cc/min during the entire dissolution. Traps of polyethylene beads and Ascarite-Drierite removed spray, water vapor and some acidic gases. Hydrogen and organic vapors were removed on CuO at 650°C, and NO_x on titanium sponge at 850°C. The Kr-Xe fission gases and respective spikes were trapped on 5-A Molecular Sieve traps in liquid nitrogen. Two collection traps were used. Gas collection was continued for at least one hour after the dissolution was considered complete, as evidenced by cessation of the evolution of ^{85}Kr from the dissolver flask and by visual examination of the dissolver flask. The average dissolution time was 10-12 h.

After dissolution, the two collection traps were removed and counted for ^{85}Kr. In no case was ^{85}Kr activity detected on the backup trap. The gases were removed from the primary collection trap and the Kr and Xe separated using gas chromatography. The individual fission gases and respective spikes were collected upon exiting from the chromatograph and analyzed by mass spectrometry.

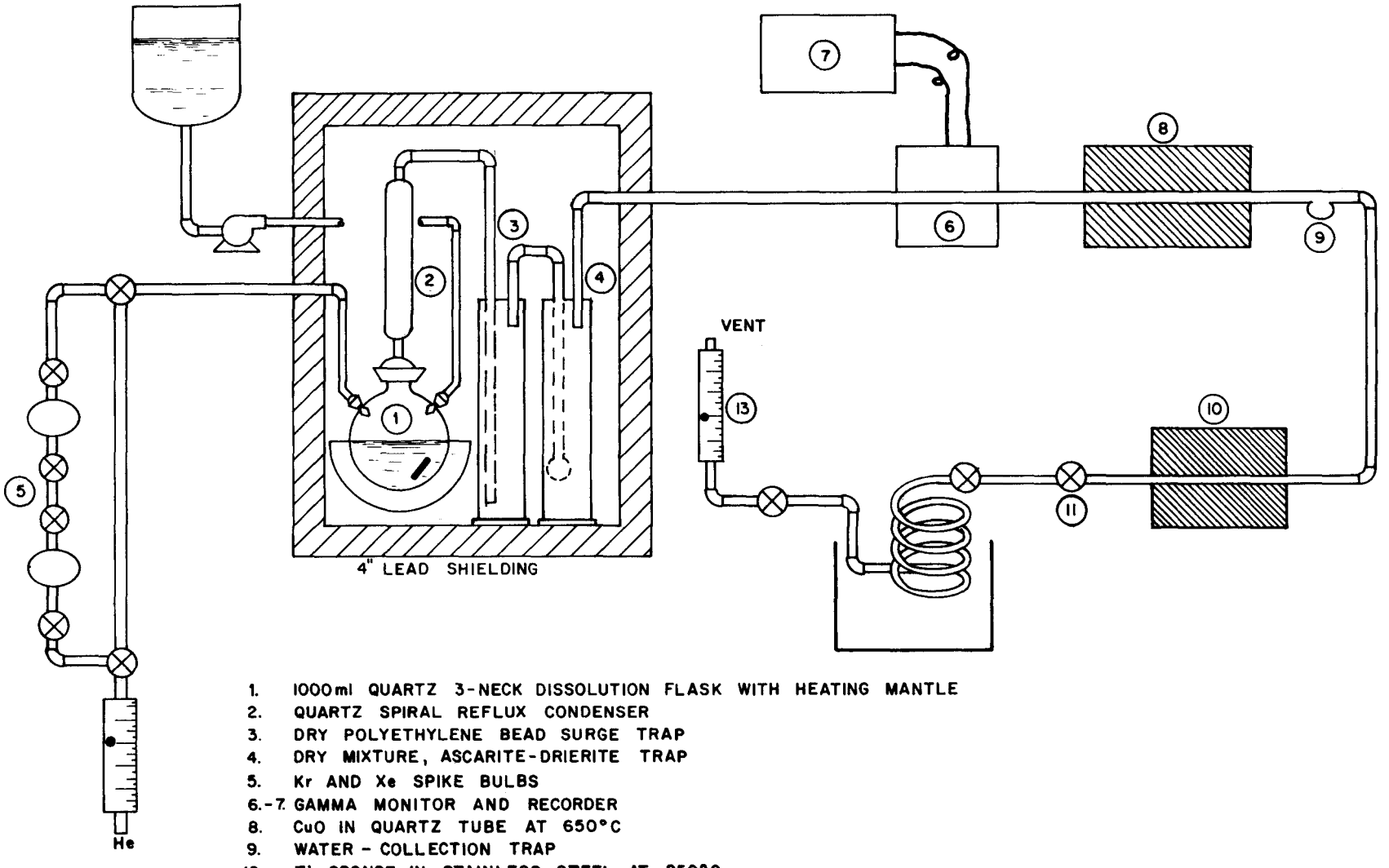

1. 1000ml QUARTZ 3-NECK DISSOLUTION FLASK WITH HEATING MANTLE
2. QUARTZ SPIRAL REFLUX CONDENSER
3. DRY POLYETHYLENE BEAD SURGE TRAP
4. DRY MIXTURE, ASCARITE-DRIERITE TRAP
5. Kr AND Xe SPIKE BULBS
6.-7. GAMMA MONITOR AND RECORDER
8. CuO IN QUARTZ TUBE AT 650°C
9. WATER - COLLECTION TRAP
10. Ti SPONGE IN STAINLESS STEEL AT 850°C
11. BY-PASS VALVE
12. MOLECULAR STEVE 5A AT -190°C (2 TRAPS)
13. OUTLET FLOWMETER AND VENT

Fig. 2 Dissolution and Gas Collection Apparatus.

Following dissolution, the sample solution was allowed to stand several hours, then filtered and weighed. The filter was counted to determine completeness of dissolution. Weighed aliquots of the sample solution were removed and mixed with weighed quantities of the respective spike for each element measured. The principal measurement technique was isotope dilution mass spectrometry. Usually, four spiked and four unspiked aliquots were analyzed for each element. Highly purified reagents were used in the chemical separations. The results are given in Sections V and VI of this report.

A brief description of the chemical separation and mass spectrometric procedures used is given in the Appendix.

III-B. SPECTRUM MONITOR SAMPLES

Seven of the 12 spectrum monitor capsules were analyzed. The nonfissionable monitors were counted using a calibrated Ge(Li) detector and a 4096 channel analyzer system. The fissionable monitors were individually dissolved, cesium chemically separated, and ^{137}Cs determined using gamma-ray analysis. Corrections for ^{137}Cs produced from other heavy nuclides were applied. Based on the determined reaction rates, the neutron spectra were characterized using the fitting code SPECTRA[3]. From these results, the mean neutron energy, median neutron energy, and the mean neutron fission energy for ^{233}U, ^{235}U, ^{238}U, ^{239}Pu, and ^{241}Pu were calculated. The results and a comparison to the expected neutron spectrum in FTR and in a conceptual 1000 MW_e LMFBR have been previously reported.[2] The values for the neutron energies given in Table I of this report were derived from these measurements.

In addition to the neutron energies given in Table I, the spectral index, $^{238}U(n,f)/^{235}U(n,f)$, for each capsule is also given. Because prior studies[6] have shown that the isotopic ratio, $^{150}Nd/^{143}Nd$, is correlated with the spectral index and hence, neutron energy, this ratio also is given in Table I.

Both the neutron spectrum data and the measured capture-to-fission ratios indicate that this irradiation was conducted in a neutron environment which approximates that expected for the FTR and a conceptual

mixed-oxide fueled 1000 MW_e LMFBR.

III-C. CAPTURE-TO-FISSION RATIO SAMPLES

The stainless steel needles containing the irradiated heavy nuclide oxides were sequentially dissolved in a mixture of HBr-HI and a mixture of HNO_3-HF. The number of fissions was determined from a ^{137}Cs analysis and the number of captures from the change in the isotopic composition of the irradiated sample or by an analysis for the amount of capture product formed. The number of fissions was corrected for fissions contributed by the neutron capture product based on the measured amount of capture product present and the estimated fission cross section. The measured capture-to-fission ratio values and comparison to the calculated values for these isotopes in the Fast Test Reactor (FFTF) have been previously reported.[2]

IV. DETERMINATION OF NUMBER OF FISSIONS

The absolute number of fissions for each of the ^{239}Pu and ^{241}Pu samples was determined by the summation technique. This is the preferred technique for samples having low burnup and is based on the fact that the sum of all of the fission product atoms in one of the peaks in the mass yield curve is equal to the number of fissions. The preferred peak for measurement is the heavy mass peak because the elements in this peak are more easily measured, and an accurate measurement of a larger fraction of this peak is possible. In this report, all yields are based on the sum of the atoms in the heavy mass peak.

Because it was impossible to measure all of the isotopes in the heavy peak, some values had to be obtained by interpolation and estimation. For those mass numbers which were not measured but were bound by measured quantities (ie, mass 141 and 153), the value was obtained by linear interpolation between the adjacent measured masses. For the region from mass 130 to 126, the values were interpolated based on the measured values of ^{131}Xe and ^{125}Sb and the general shape of the mass yield curve in this region for thermal fission. For the region 126 to one-half the mass of the compound target less neutron emission, the

values were estimated using thermal data as a guide and adjusting for an increase in the valley yields. The number of atoms in the region from 155 to 160 was estimated by extrapolating the measured mass yield curve from mass 154 to 160. The fractions of the heavy mass peak derived by each of these techniques and the assigned uncertainties for a typical sample are given in Table III.

The actual measured, interpolated, extrapolated, and estimated number of atoms and respective uncertainties for each of the analyzed samples is given in Tables XV, XVI, XVII, and XIX for the ^{239}Pu samples and Tables XXXI and XXXII for the ^{241}Pu samples.

V. ^{239}Pu FAST FISSION YIELDS

Four encapsulated samples of highly enriched ^{239}Pu oxide were irradiated and analyzed. The location of the samples in the irradiation assembly is shown in Figure 1. Of the four samples, three (Nos. 5, 24, and 26) were clustered about the reactor mid-plane and were exposed to essentially the same neutron spectrum (Table I). The other sample, No. 35, was located out of the core region in the axial blanket and exposed to a much softer spectrum. In the treatment of the data, the results from the three capsules were pooled and considered representative of a common neutron spectrum, while capsule 35 was treated separately, representative of a spectrum intermediate between the other three and thermal. Based on the measured abundance of ^{135}Cs, there is no evidence of a significant thermal neutron component in this axial blanket position. The neutron spectra, characterized by several different indices for each capsule are given in Table I.

V-A. ISOTOPIC COMPOSITION OF FISSION PRODUCT ELEMENTS

The isotopic composition for each of the fission product elements measured is given in Tables IV through XIV. In all cases, except for krypton and xenon, the values are based on four individual unspiked analyses. For each of the reported isotopic abundances, the stated uncertainty is the standard deviation of the mean for the multiple measurements and only depicts the random error of the measurements.

TABLE III

COMPONENTS AND ERRORS RELATIVE
TO DETERMINING THE NUMBER OF FISSIONS

	^{239}Pu		^{241}Pu	
	% Total	Relative Error,%	% Total	Relative Error, %
Measured Atoms				
Sb	0.133	11.1	0.066	11.1
Xe	23.90	1.8	22.31	1.2
Cs	21.23	0.5	20.60	0.5
Ba	6.11	0.8	6.43	0.6
La	5.45	2.1	6.33	2.8
Ce	9.98	1.1	10.13	1.2
Nd	16.16	0.9	17.99	0.7
Sm	4.81	1.4	5.66	0.8
Σ Measured Atoms	87.77	0.6	89.51	0.4
Linear Interpolation, Mass 141	4.99	5.2	5.06	5.2
Linear Interpolation, Mass 153	0.425	5.2	0.533	5.2
Interpolation, Mass 130-126	6.13	8.0	4.01	7.0
Extrapolation, Mass 155-160	0.40	25.0	0.17	25.0
Estimation, Mass 124-119	0.28	25.0	0.71	25.0
TOTAL	100.00%	0.8%	100.00%	0.6%

For krypton and xenon, only one sample is collected and analyzed. The mean of the results obtained from three of the capsules was calculated and the stated uncertainty is the standard deviation of the mean. Because capsule 35 was irradiated in a different neutron spectrum, it is treated separately.

Also listed in these tables is the isotopic composition of the same fission product elements resulting from thermal neutron fission. Two reference sources were used. One is Walker's compilation[4] which lists all mass spectrometric fission product measurements reported through 1973, and the other is a listing of recent results reported by this laboratory[5] for the measurement of the isotopic composition of krypton, rubidium, xenon, cesium, and neodymium.

The extensive listing of the unspiked isotopic data is important because it is more precise and accurate than fission yield data. Thus, a more meaningful comparison to other reported data is possible, especially with respect to the changes in the relative isotopic abundances as a function of neutron energy. In many cases, these changes are more vividly shown by ratioing the isotopic abundance of the extreme mass numbers of the individual fission product element. If the isotopic composition of a given fission product element changes, then the fission yields also must show a change. However, no change in the isotopic composition does not preclude a change in the fission yields, because the yields may all change by the same relative amount.

V-B. ABSOLUTE FISSION YIELDS

The measured and estimated number of atoms for each individual fission product nuclide and the sum of the atoms for a given region of the mass yield curve for each of the four analyzed capsules is given in Tables XV, XVI, XVII, and XIX. Also given for each capsule is the total number of fissions based on the sum of the fission product atoms in the heavy mass peak, and the fission yield of each nuclide which was obtained by dividing the measured number of atoms of that nuclide by the sum of the atoms in the heavy mass peak.

The results are summarized in Table XVIII for the three capsules irradiated in a like spectrum, and in Table XIX for capsule 35, which was in a significantly different spectrum.

V-B-1. Heavy Mass Peak

V-B-1-a. Mass Region 119-124. The number of atoms in the mass region 119-124 was estimated based on the measured value for ^{125}Sb and a comparison to the shape of the mass yield curve in this region for thermal fission. Allowing for an increase in the yields of the valley nuclides, this region of the heavy mass peak equals ∿0.28% of the total. A 25% relative uncertainty was assigned to this value.

V-B-1-b. Mass 125. The atoms of mass 125 were determined from a radiochemical measurement for ^{125}Sb.

V-B-1-c. Mass Region 126-130. The number of atoms for each mass number was obtained by interpolation. A smooth function was assumed between the measured values for ^{125}Sb and ^{131}Xe. The shape of the thermal fission yield curve was used as a guide. The sum of the atoms in this region is ∿6.1% of the total atoms in the heavy mass peak. The uncertainty on the sum, ∿8.0% relative, was obtained assuming a 10% relative systematic error for each individual mass number estimate and includes the error due to the uncertainty in the measured ^{125}Sb and xenon values.

V-B-1-d. Xenon (Mass 131, 132, 134, 136). A slight, but significant difference is shown (Table IV) for the isotopic composition of xenon produced by fast fission compared to thermal fission. For the ratio $^{131}Xe/^{134}Xe$, the value for fast fission is ∿3% greater than for thermal fission. This is not unreasonable because mass 131 lies on the light shoulder of the heavy mass peak and is influenced by an increase in the fission yields of the valley nuclides with increasing neutron energy. To compare the fast to thermal yields, the data have been renormalized to include only ^{131}Xe, ^{132}Xe, and ^{134}Xe.

TABLE IV

ISOTOPIC COMPOSITION OF XENON
FROM ^{239}Pu FAST AND THERMAL FISSION

	FAST FISSION					
	CAPSULE					
Isotope	5	24	26	$\bar{X}/\sigma_{\bar{X}}$	Capsule 35	Thermal[5] Fission
^{131}Xe	0.1642	0.1640	0.1641	0.1641 ±0.0001	0.1599	
^{132}Xe	0.2258	0.2248	0.2262	0.2256 ±0.0004	0.2291	
^{134}Xe	0.3156	0.3163	0.3155	0.3158 ±0.0003	0.3100	
^{136}Xe	0.2938	0.2946	0.2937	0.2940 ±0.0003	0.2952	
$^{131}Xe/^{134}Xe$	0.5203	0.5185	0.5201	0.5196 ±0.0006	0.5158	0.5057 ±0.0004
$^{131}Xe/^{136}Xe$	0.5589	0.5567	0.5587	0.5581 ±0.0007	0.5417	
Renormalized to include only masses 131, 132, and 134.						
^{131}Xe	0.2327	0.2326	0.2326	0.2326 ±0.0001	0.2287	0.2289 ±0.0002
^{132}Xe	0.3200	0.3188	0.3204	0.3197 ±0.0005	0.3278	0.3185 ±0.0002
^{134}Xe	0.4472	0.4486	0.4470	0.4476 ±0.0005	0.4436	0.4526 ±0.0003

V-B-1-e. Cesium (Mass 133, 135, 137). Cesium which lies in the center of the heavy mass peak shows little or no significant change in its isotopic composition (Table V) between fast and thermal fission. To provide a comparison to thermal values, the data have been renormalized to include only ^{133}Cs and ^{137}Cs. The absolute value for the number

of ^{137}Cs atoms was obtained by summing the measured atoms of ^{137}Cs and ^{137}Ba. Also, the number of 137 atoms was calculated based on the independently measured number of atoms of ^{137}Cs and ^{137}Ba using a half-life value of 30.1y for ^{137}Cs. Excellent agreement was obtained for the number of mass 137 atoms, indicating no serious natural contamination problem for either the cesium or barium measurements.

TABLE V

ISOTOPIC COMPOSITION OF CESIUM
FROM ^{239}Pu FAST AND THERMAL FISSION

	FAST FISSION					
	CAPSULE					
Isotope	5	24	26	$\bar{X}/\sigma_{\bar{X}}$	Capsule 35	Thermal[5] Fission
^{133}Cs	0.3303 ±0.0001	0.3300 ±0.0001	0.3315 ±0.0001	0.3306 ±0.0005	0.3315 ±0.0001	
^{135}Cs	0.3576 ±0.0001	0.3574 ±0.0001	0.3576 ±0.0001	0.3575 ±0.0001	0.3571 ±0.0001	
^{137}Cs	0.3120 ±0.0001	0.3126 ±0.0001	0.3110 ±0.0001	0.3119 ±0.0005	0.3114 ±0.0001	
$^{133}Cs/^{137}Cs$	1.059	1.056	1.066	1.060 ±0.004	1.065	1.0648 ±0.0002
Renormalized to include only masses 133 and 137.						
^{133}Cs	0.5142 ±0.0002	0.5135 ±0.0002	0.5160 ±0.0002	0.5146 ±0.0007	0.5156 ±0.0002	0.5157 ±0.0002
^{137}Cs	0.4858 ±0.0002	0.4865 ±0.0002	0.4840 ±0.0002	0.4854 ±0.0007	0.4844 ±0.0002	0.4843 ±0.0002

V-B-1-f. Barium (Mass 138). The atoms of mass 138 were determined from an analysis of barium. Although barium is a common natural contaminant, it did not appear to present a serious problem in this work based on the agreement obtained for the atoms of mass 137 determined independently from ^{137}Cs and ^{137}Ba (see Section V-B-1-e). In this case, the

abundance of ^{137}Ba was ∿10 times less than the atoms of ^{138}Ba and would have reflected even a small natural barium contamination problem.

V-B-1-g. Lanthanum (Mass 139). The only stable fission product isotope of lanthanum is mass 139. Unfortunately, it has a natural abundance of 99.91% which can cause serious natural contamination problems. The only other stable natural occurring isotope is 138, having a natural abundance of 0.09; hence, the use of mass 138 as a monitor for natural contamination is subject to significant errors. In addition, the spike isotope, ^{138}La, was only enriched to ∿20% resulting in significant corrections to the measured 139 mass. For these reasons, the reported atoms of fission product ^{139}La carries the largest uncertainty of all of the fission products measured.

V-B-1-h. Cerium (Mass 140, 142). Three isotopes of cerium, mass 140, 142, and 144, were measured. The atoms of ^{144}Ce are summed with ^{144}Nd to give a total 144 mass. For fast fission, the ratio $^{140}Ce/^{142}Ce$ shows (Table VI) about a 1% change from that produced by thermal fission.[4]

TABLE VI

ISOTOPIC COMPOSITION OF CERIUM
FROM ^{239}Pu FAST AND THERMAL FISSION

	FAST FISSION					
	CAPSULE					
Isotope	5	24	26	$\bar{X}/\sigma_{\bar{X}}$	Capsule 35	Thermal[4] Fission
^{140}Ce	0.5233 ±0.0001	0.5246 ±0.0002	0.5276 ±0.0010	0.5252 ±0.0013	0.5275 ±0.0003	0.5278 ±0.0026
^{142}Ce	0.4767 ±0.0001	0.4754 ±0.0002	0.4724 ±0.0010	0.4748 ±0.0013	0.4725 ±0.0004	0.4722 ±0.0038
$^{140}Ce/^{142}Ce$	1.098	1.103	1.117	1.106 ±0.006	1.116	1.118

For many years, difficulties have been experienced in the accurate mass spectrometric analysis of cerium because of the inability to accurately measure the small abundance of ^{136}Ce and ^{138}Ce isotopes in the presence of large amounts of ^{140}Ce and ^{142}Ce. This has resulted in relatively poor corrections for the natural cerium component, which is based on ^{136}Ce. The ^{136}Ce abundance in natural cerium is 0.19%. Because the ratio of $^{140}Ce/^{142}Ce$ in natural cerium is $\sim$8, the inability to reliably correct for natural contamination introduces a significant uncertainty in the measured atoms of fission product cerium, especially in ^{140}Ce. A newly developed mass spectrometric measurement technique, which is discussed in the Appendix, now permits a more accurate measurement of ^{136}Ce, and hence, more accurate fission product cerium data. (See section V-B-1-j for confirmatory evidence.)

V-B-1-i. Mass 141. The atoms of mass 141 were obtained by linear interpolation between the measured atoms of ^{140}Ce and ^{142}Ce. The number of mass 141 atoms comprise $\sim$5.0% of the total heavy mass peak. The propagated relative uncertainty is 5.2% which includes an assigned 5% relative systematic error and the error due to the uncertainty in the number of measured ^{140}Ce and ^{142}Ce atoms.

V-B-1-j. Neodymium (Mass 143, 144, 145, 146, 148, 150). The isotopic composition of the neodymium isotopes for the four capsules irradiated in EBR-II and for thermal fission[5] is given in Table VII. The value for 144 is based on the sum of the measured atoms of ^{144}Nd plus ^{144}Ce. Because the chemical separation and mass spectrometric measurements were conducted at essentially the same time, little or no significant decay corrections were involved. To validate the ^{144}Ce measurement, the total atom abundance of the 144 mass chain was calculated from the ^{144}Ce analysis using a half-life of 284.4d. If this measurement were in error, the total mass 144 would be different from that determined solely from ^{144}Nd because a significant decay correction is required to be applied to the ^{144}Ce value. No serious discrepancies were observed.

The change in the neodymium isotopic composition and hence, fission yields, is an important consideration in the use of the neodymium isotopes as monitors for the number of fissions in the determination of nuclear fuel burnup. From the data given in Table VII, it is quite evident that the isotopic abundance of the light neodymium isotopes decreases with increasing neutron energy while the isotopic abundance of ^{150}Nd increases with neutron energy. This is not surprising because the wings of the mass yield curve tend to broaden with increasing neutron energy and the peak intensity decreases.

Previously, it has been shown[6] that the $^{150}Nd/^{143}Nd$ ratio for ^{235}U fission is dependent upon neutron energy and, therefore, it also may be a useful spectral index monitor. For this reason, the $^{150}Nd/^{143}Nd$ ratio has been included with the spectral information given in Table I.

TABLE VII

ISOTOPIC COMPOSITION OF NEODYMIUM
FROM ^{239}Pu FAST AND THERMAL FISSION

	FAST FISSION					
	CAPSULE					
Isotope	5	24	26	$\bar{X}/\sigma_{\bar{X}}$	Capsule 35	Thermal[5] Fission
^{143}Nd	0.2704 ±0.0004	0.2699 ±0.0002	0.2702 ±0.0001	0.2702 ±0.0001	0.2713 ±0.0002	0.2723 ±0.0001
^{144}Nd	0.2291 ±0.0001	0.2293 ±0.0001	0.2297 ±0.0001	0.2294 ±0.0002	0.2304 ±0.0001	0.2312 ±0.0001
^{145}Nd	0.1859 ±0.0001	0.1857 ±0.0001	0.1856 ±0.0001	0.1857 ±0.0001	0.1852 ±0.0001	0.1848 ±0.0001
^{146}Nd	0.1521 ±0.0001	0.1522 ±0.0001	0.1520 ±0.0001	0.1521 ±0.0001	0.1512 ±0.0002	0.1510 ±0.0001
^{148}Nd	0.1019 ±0.0001	0.1022 ±0.0001	0.1020 ±0.0001	0.1020 ±0.0001	0.1018 ±0.0001	0.1012 ±0.0001
^{150}Nd	0.0605 ±0.0001	0.0607 ±0.0001	0.0605 ±0.0001	0.0606 ±0.0001	0.0601 ±0.0001	0.05944 ±0.00027
$^{150}Nd/^{143}Nd$	0.2238	0.2248	0.2239	0.2242 ±0.0003	0.2214	0.2183 ±0.0003

V-B-1-k. Samarium (Mass 147, 149, 151, 152, 154). The isotopic composition of samarium produced by fast and thermal fission[4] is given in Table VIII. Comparison of the fast and thermal data is difficult because many corrections[4] have been applied to the thermal data to account for neutron capture. One item in particular, is the abundance of mass 154. It is believed that the value for thermal fission may be too high, because we would have expected the abundance of ^{154}Sm to be greater for fast fission than for thermal fission. This question may be resolved in the continuation of our program to remeasure the thermal fission yields.[5] None of the fast fission samarium data have been corrected for neutron capture because the irradiation was of short duration and there was no detectable thermal neutron component.

The values for ^{147}Sm were corrected for decay using a half-life of 2.623y for ^{147}Pm. For ^{151}Sm, the correction was based on a half-life of 93y.

TABLE VIII

ISOTOPIC COMPOSITION OF SAMARIUM
FROM ^{239}Pu FAST AND THERMAL FISSION

	FAST FISSION					
	CAPSULE					
Isotope	5	24	26	$\bar{X}/\sigma_{\bar{X}}$	Capsule 35	Thermal[4] Fission
^{147}Sm	0.4103 ±0.0002	0.4101 ±0.0006	0.4111 ±0.0003	0.4105 ±0.0003	0.4132 ±0.0004	0.4170 ±0.0008
^{149}Sm	0.2534 ±0.0002	0.2534 ±0.0003	0.2535 ±0.0001	0.2534 ±0.0001	0.2533 ±0.0002	0.2512 ±0.0050
^{151}Sm	0.1598 ±0.0004	0.1606 ±0.0003	0.1603 ±0.0003	0.1602 ±0.0002	0.1587 ±0.0002	0.1570 ±0.0031
^{152}Sm	0.1219 ±0.0001	0.1216 ±0.0003	0.1211 ±0.0002	0.1215 ±0.0002	0.1209 ±0.0002	0.1195 ±0.0024
^{154}Sm	0.0546 ±0.0001	0.0543 ±0.0001	0.0540 ±0.0001	0.0543 ±0.0002	0.0539 ±0.0002	0.0551 ±0.0011
$^{147}Sm/^{154}Sm$	7.515	7.552	7.613	7.560 ±0.029	7.666	7.568
$^{147}Sm/^{152}Sm$	3.366	3.373	3.395	3.378 ±0.009	3.418	3.490

V-B-1-ℓ. Mass 153. The atoms of mass 153 were obtained by linear interpolation between the measured atoms of ^{152}Sm and ^{154}Sm. The number of mass 153 atoms comprise ∿0.42% of the total heavy mass peak. The propagated uncertainty is 5.2% relative, which includes an assigned 5% relative systematic error for mass 153, and the error due to the uncertainty in the measured samarium values.

V-B-1-m. Mass Region 156 to 160. The number of atoms in this mass region was obtained by extrapolating the measured number of atoms in the 150-154 mass region to mass 160. This mass region comprises ∿0.4% of the total heavy mass peak and a 25% relative uncertainty has been assigned to the value.

V-B-2. Light Mass Peak

The yields for all measured isotopes were obtained by dividing the number of atoms of each measured mass by the sum of the atoms in the heavy mass peak.

V-B-2-a. Mass Region 75 to 82. The number of atoms in the mass region 75 through 82 was obtained by extrapolating the measured number of atoms of the krypton isotopes to mass 75. The region from mass 75 to 80 is listed as an individual value. Mass 81 and 82 are treated as separate values and are listed as such.

V-B-2-b. Krypton (Mass 83, 84, 86). The isotopic composition of krypton produced by fast and thermal fission[5] is given in Table IX. The ratio of $^{86}Kr/^{83}Kr$ for fast fission is significantly different (∿3%) from that for thermal fission and in the direction which supports broadening of the wings in this region of the mass yield curve with increasing neutron energy.

Krypton-85 is not included in the Table IX compilation because ∿80% of this mass number exists in the form of ^{85}Rb. The measured atoms of ^{85}Kr are summed with those of ^{85}Rb and given in Table X.

TABLE IX

ISOTOPIC COMPOSITION OF KRYPTON
FROM ^{239}Pu FAST AND THERMAL FISSION

	FAST FISSION					
	CAPSULE					
Isotope	5	24	26	$\overline{X}/\sigma_{\overline{X}}$	Capsule 35	Thermal[5] Fission
^{83}Kr	0.1964	0.1961	0.1964	0.1963 ±0.0001	0.1945	0.1927 ±0.0002
^{84}Kr	0.3104	0.3114	0.3124	0.3114 ±0.0006	0.3108	0.3100 ±0.0005
^{86}Kr	0.4933	0.4925	0.4912	0.4923 ±0.0006	0.4946	0.4973 ±0.0003
$^{86}Kr/^{83}Kr$	2.512	2.511	2.501	2.508 ±0.004	2.543	2.581

V-B-2-c. Rubidium (Mass 85, 87). The relative isotopic composition of rubidium resulting from fast and thermal fission is given in Table X. The abundance of mass 85 was obtained by summing the measured atoms of ^{85}Kr and ^{85}Rb. The isotopic ratio, $^{85}Rb/^{87}Rb$, is relatively insensitive to changes in neutron energy.

TABLE X

ISOTOPIC COMPOSITION OF RUBIDIUM
FROM ^{239}Pu FAST AND THERMAL FISSION

	FAST FISSION					
	CAPSULE					
Isotope	5	24	26	$\overline{X}/\sigma_{\overline{X}}$	Capsule 35	Thermal[5] Fission
$^{85}Kr+^{85}Rb$	0.3657	0.3646	0.3666	0.3656 ±0.0006	0.3711	0.3650 ±0.0004
^{87}Rb	0.6343	0.6354	0.6334	0.6344 ±0.0006	0.6289	0.6350 ±0.0004
$^{85}Rb/^{87}Rb$	0.5765	0.5738	0.5788	0.5764 ±0.0014	0.5901	0.5748

V-B-2-d. Strontium (Mass 88, 90). The isotopic composition for strontium produced by fast and thermal fission is given in Table XI. The number of mass 90 atoms is the sum of the measured ^{90}Sr and ^{90}Zr atoms. The change in the isotopic ratio $^{88}Sr/^{90}Sr$ with neutron energy is less than 1%.

TABLE XI

ISOTOPIC COMPOSITION OF STRONTIUM
FROM ^{239}Pu FAST AND THERMAL FISSION

	FAST FISSION					
	CAPSULE					
Isotope	5	24	26	$\bar{X}/\sigma_{\bar{X}}$	Capsule 35	Thermal[4] Fission
^{88}Sr	0.3939	0.3950	0.3952	0.3947 ±0.0004	0.3934	0.3932 ±0.0020
^{90}Sr	0.6061	0.6050	0.6048	0.6053 ±0.0004	0.6066	0.6068 ±0.0018
$^{88}Sr/^{90}Sr$	0.6499	0.6529	0.6534	0.6521 ±0.0011	0.6485	0.6469

V-B-2-e. Mass 89. The atoms of mass 89 were obtained by linear interpolation between the measured atoms of ^{88}Sr and ^{90}Sr. The propagated uncertainty associated with this value is 5.2% relative, which includes an assigned 5% relative systematic error and the error due to the uncertainty in the measured strontium atoms.

V-B-2-f. Zirconium (Mass 91, 92, 93, 94, 96). Table XII gives the isotopic composition of zirconium produced from fast and thermal fission. Zirconium proved to be one of the more difficult analyses because significant corrections for natural contamination were required. The source of the natural contamination is believed to be the quartz dissolution flasks which are normally annealed in a zirconia lined furnace in the manufacturing process.

Being near the center of the light mass peak, the isotopic composition of fission product zirconium is little affected by changes in neutron energy.

TABLE XII

ISOTOPIC COMPOSITION OF ZIRCONIUM
FROM ^{239}Pu FAST AND THERMAL FISSION

	FAST FISSION					
	CAPSULE					
Isotope	5	24	26	$\bar{X}/\sigma_{\bar{X}}$	Capsule 35	Thermal[4] Fission
^{91}Zr	0.1347 ±0.0003	0.1349 ±0.0003	0.1340 ±0.0003	0.1345 ±0.0003	0.1335 ±0.0004	0.1327 ±0.0014
^{92}Zr	0.1636 ±0.0002	0.1639 ±0.0002	0.1664 ±0.0012	0.1646 ±0.0009	0.1636 ±0.0002	0.1615 ±0.0002
^{93}Zr	0.2062 ±0.0003	0.2064 ±0.0001	0.2053 ±0.0015	0.2060 ±0.0003	0.2052 ±0.0003	0.2052 ±0.0006
^{94}Zr	0.2330 ±0.0007	0.2321 ±0.0002	0.2311 ±0.0005	0.2321 0.0005	0.2325 ±0.0002	0.2329 ±0.0018
^{96}Zr	0.2625 ±0.0003	0.2628 ±0.0005	0.2632 ±0.0008	0.2628 ±0.0002	0.2651 ±0.0004	0.2677 ±0.0008
$^{91}Zr/^{96}Zr$	0.5131	0.5133	0.5091	0.5118 ±0.0014	0.5006	0.4957

V-B-2-g. Molybdenum (Mass 95, 97, 98, 100). The isotopic composition of molybdenum for fast and thermal fission is given in Table XIII. Again, little change in the isotopic composition as a function of neutron energy is shown.

V-B-2-h. Mass 99. The atoms of mass 99 were determined by linear interpolation between the measured atoms of ^{98}Mo and ^{100}Mo. The propagated uncertainty associated with this value is 5.2% relative, which includes an assigned 5% relative systematic error and the error due to the uncertainty in the measured molybdenum atoms.

TABLE XIII

ISOTOPIC COMPOSITION OF MOLYBDENUM
FROM ^{239}Pu FAST AND THERMAL FISSION

	FAST FISSION					
	CAPSULE					
Isotope	5	24	26	$\bar{X}/\sigma_{\bar{X}}$	Capsule 35	Thermal[4] Fission
^{95}Mo	0.2102 ±0.0002	0.2113 ±0.0002	0.2097 ±0.0008	0.2104 ±0.0005	0.2128 ±0.0004	0.2132
^{97}Mo	0.2385 ±0.0004	0.2388 |0.0002	0.2394 ±0.0003	0.2389 0.0003	0.2344 ±0.0003	0.2386
^{98}Mo	0.2529 ±0.0004	0.2539 ±0.0003	0.2532 ±0.0003	0.2533 ±0.0003	0.2613 ±0.0001	0.2485
^{100}Mo	0.2984 ±0.0005	0.2960 ±0.0002	0.2977 ±0.0008	0.2974 ±0.0007	0.2916 ±0.0005	0.2998
$^{95}Mo/^{100}Mo$	0.7044	0.7139	0.7044	0.7076 ±0.0032	0.7298	0.7111

V-B-2-i. Ruthenium (Mass 101, 102, 103, 104, 105, 106). The measured isotopic composition of ruthenium for mass numbers 101, 102, 104, and 106 for fast and thermal fission[4] is given in Table XIV. It is difficult to make reliable comments concerning the ruthenium isotopic composition relative to neutron energy because large uncertainties are associated with the thermal data, especially for mass 106, which is normally subjected to large in-pile and out-pile decay corrections. In addition, it is the least abundant isotope and thus, more difficult to measure. In this work, the largest uncertainties also are associated with the ^{106}Ru value.

TABLE XIV

ISOTOPIC COMPOSITION OF RUTHENIUM
FROM ^{239}Pu FAST AND THERMAL FISSION

	FAST FISSION					
	CAPSULE					
Isotope	5	24	26	$\bar{X}\sigma_{\bar{X}}$	CAPSULE 35	Thermal[4] Fission
^{101}Ru	0.2728 ±0.0002	0.2715 ±0.0008	0.2722 ±0.0003	0.2722 ±0.0004	0.2713 ±0.0002	0.2656 ±0.0018
^{102}Ru	0.2759 ±0.0001	0.2769 ±0.0005	0.2766 ±0.0001	0.2764 ±0.0003	0.2769 ±0.0001	0.2705 ±0.0032
^{104}Ru	0.2704 ±0.0001	0.2729 ±0.0002	0.2725 ±0.0004	0.2719 ±0.0008	0.2737 ±0.0003	0.2683 ±0.0034
^{106}Ru	0.1809 ±0.0023	0.1787 ±0.0016	0.1786 ±0.0054	0.1794 ±0.0008	0.1781 ±0.00013	0.1956 ±0.0084
$^{101}Ru/^{104}Ru$	1.009	0.9945	0.9991	1.0009 ±0.0043	0.9916	0.9899
$^{101}Ru/^{106}Ru$	1.508	1.519	1.524	1.517 ±0.006	1.523	1.358

In the dissolution of our capsules, it was determined that varying amounts of ruthenium plated out on the wall of the dissolver or precipitated from the solution. Thus, the actual measured number of atoms was not indicative of the total fission product ruthenium concentration. Two methods were used to correct for this loss. One involved gamma counting all of the dissolver components and a fraction of the dissolver solution to determine the fractional loss, and the other involved a calculational process. Because adequate geometry factors were not available for the gamma counting technique and large uncertainties in the results were obtained, it was decided to use the calculational approach. This method assumes no isotopic fractionation in the plate-out process and that the isotopic composition of the dissolved ruthenium is representative of the total fission product ruthenium.

To obtain the total ruthenium concentration, all of the measured and estimated atoms in the light peak, except those in the mass region 101 through 106 inclusive, were summed and subtracted from the total number of atoms in the heavy mass peak. This difference, the total atoms in the mass region 101 through 106, was subsequently allocated to each mass number based on the measured ruthenium isotopic composition. Because mass 103 and 105 were not measured, the relative abundance for each was obtained by linear interpolation between the measured values for ^{102}Ru and ^{104}Ru, and between ^{104}Ru and ^{106}Ru, respectively. The propagated error calculated for mass 103 and 105 is 7.4% relative and includes an assigned systematic error of 7% and the error due to the uncertainty in the measured ruthenium.

This method is extremely sensitive to errors in the sum of the atoms in each mass peak; however, the random error of the mean for the ruthenium fission yields calculated by this technique for the three capsules is only ∿1%. The total propagated errors for the fission yields determined by this technique range from ∿2-7% and are given in Tables XV through XX. The correction factors for the amount of ruthenium plate-out determined by this technique are 1.118 for capsule 5, 1.032 for capsule 24, 1.183 for capsule 26, and 1.018 for capsule 35. The fact that the simple random error associated with the mean of the yields is small, ∿2% lends validity to this technique.

V-B-2-j. Mass 107, 108, 109, 110. The number of atoms for these mass numbers was obtained by interpolation and extrapolation. As a guide, a fission yield of 0.3% for mass 111 at 500 keV determined by Cunninghame and Willis[7] was used. The assigned error associated with the number of atoms for each mass number is 15%.

V-B-2-k. Mass 111. Recently Cunninghame and Willis[7] reported the fission yield of ^{111}Ag for ^{239}Pu fission as a function of neutron energy, based on radiochemical measurements and fissioning by monoenergetic neutrons. Based on a reported linear correlation of ^{111}Ag fission yields for neutron energies ranging from 130-1700 keV, a yield of 0.3% at ∿500 keV was selected. To obtain the number of mass 111 atoms for each capsule, the sum of the atoms in the heavy mass peak

was multiplied by 0.003. The assigned error associated with the number of mass 111 atoms is 15% relative.

V-B-2-ℓ. Mass 112-118. The number of atoms in this mass region was obtained by estimation, attempting to account for the increase in the abundance of the valley nuclides with increasing neutron energy. A 25% relative uncertainty was assigned to this value.

V-C. ERROR ANALYSIS

The standard deviation associated with each reported fission yield is given in Tables XV-XXI and includes allowances for known sources of systematic errors. The standard deviation was calculated by first approximating the functions used to calculate the fission yields, by the linear terms of the Taylor series expansion, and then applying the usual method of calculating the standard deviation of a linear sum of random variables. The procedure consisted of five distinct steps. First, the propagated standard deviation of the measured number of atoms of each element was calculated. This computation included the systematic effect of uncertainty in the spike concentrations, the random mass spectrometer errors in the spike, natural, fission product, and mixed spike-fission product isotopic fractions, and the Kr and Xe spike volume uncertainties. One recognized uncertainty not included is the systematic error in the element concentration resulting from systematic errors in the mass spectrometer. Second, the standard deviation of the total number of atoms in the heavy peak was calculated using the above standard deviations for the measured atoms and estimated atoms. Third, the standard deviation of each yield from each capsule then was calculated using the standard deviations of the total number of fissions, the atoms of the specific element, and the fraction of the specific isotope. The standard deviation of the isotopic fractions includes the random mass spectrometer errors and the estimated systematic uncertainty in the mass spectrometer. Fourth, the standard deviations of the total number of fissions, atoms of each element, and isotopic yields for each capsule, were calculated using the observed random error in the element yields. Finally, the standard deviation of the average yield from all capsules was calculated considering the effects of the systematic and random errors.

TABLE XV

MEASURED ATOMS AND FAST FISSION YIELDS FOR ^{239}Pu - CAPSULE 5

HEAVY MASS PEAK			LIGHT MASS PEAK		
Mass No.	Atoms x10^{17}	Fission Yield	Mass No.	Atoms x10^{17}	Fission Yield
119-124	0.38 ± 0.1	0.28 ± 0.07	75-80	0.23 ± 0.05	0.17 ± 0.04
125-Sb	0.180 ± 0.020	0.13 ± 0.02	81	0.19 ± 0.02	0.14 ± 0.01
126	0.39 ± 0.06	0.29 ± 0.04	82	0.30 ± 0.03	0.22 ± 0.02
127	0.74 ± 0.11	0.55 ± 0.08	83-Kr	0.421 ± 0.004	0.312 ± 0.004
128	1.40 ± 0.17	1.04 ± 0.09	84-Kr	0.665 ± 0.005	0.492 ± 0.006
129	2.25 ± 0.23	1.67 ± 0.18	85-Kr+Rb	0.799 ± 0.009	0.592 ± 0.007
130	3.50 ± 0.37	2.59 ± 0.26	86-Kr	1.057 ± 0.009	0.783 ± 0.009
131-Xe	5.277 ± 0.099	3.908 ± 0.065	87-Rb	1.387 ± 0.017	1.027 ± 0.015
132-Xe	7.257 ± 0.135	5.374 ± 0.100	88-Sr	1.761 ± 0.022	1.304 ± 0.019
133-Cs	9.468 ± 0.056	7.012 ± 0.063	89	2.234 ± 0.117	1.655 ± 0.088
134-Xe	10.143 ± 0.185	7.512 ± 0.107	90-Sr	2.709 ± 0.033	2.006 ± 0.027
135-Cs	10.252 ± 0.053	7.592 ± 0.065	91-Zr	3.319 ± 0.052	2.458 ± 0.043
136-Xe	9.592 ± 0.177	7.104 ± 0.102	92-Zr	4.032 ± 0.062	2.986 ± 0.051
137-Cs+Ba	8.941 ± 0.055	6.622 ± 0.061	93-Zr	5.083 ± 0.077	3.765 ± 0.064
138-Ba	8.252 ± 0.066	6.111 ± 0.065	94-Zr	5.742 ± 0.088	4.253 ± 0.073
139-La	7.357 ± 0.156	5.448 ± 0.117	95-Mo	6.317 ± 0.067	4.678 ± 0.061
140-Ce	7.054 ± 0.074	5.224 ± 0.077	96-Zr	6.471 ± 0.101	4.792 ± 0.083
141	6.741 ± 0.356	4.992 ± 0.252	97-Mo	7.167 ± 0.071	5.308 ± 0.066
142-Ce	6.428 ± 0.067	4.760 ± 0.055	98-Mo	7.600 ± 0.074	5.628 ± 0.070
143-Nd	5.901 ± 0.057	4.370 ± 0.048	99	8.285 ± 0.431	6.136 ± 0.322
144-Nd+Ce	5.001 ± 0.046	3.704 ± 0.038	100-Mo	8.968 ± 0.093	6.641 ± 0.085
145-Nd	4.058 ± 0.037	3.005 ± 0.032	101-Ru	9.162 ± 0.255	6.785 ± 0.145
146-Nd	3.320 ± 0.030	2.459 ± 0.027	102-Ru	9.267 ± 0.233	6.863 ± 0.124
147-Sm	2.663 ± 0.039	1.972 ± 0.031	103	9.175 ± 0.675	6.794 ± 0.491
148-Nd	2.224 ± 0.023	1.647 ± 0.020	104-Ru	9.081 ± 0.191	6.725 ± 0.104
149-Sm	1.644 ± 0.023	1.218 ± 0.019	105	7.579 ± 0.557	5.613 ± 0.405
150-Nd	1.321 ± 0.016	0.978 ± 0.014	106-Ru	6.076 ± 0.151	4.500 ± 0.092
151-Sm	1.037 ± 0.015	0.768 ± 0.014	107	4.05 ± 0.61	3.00 ± 0.45
152-Sm	0.791 ± 0.011	0.586 ± 0.010	108	2.50 ± 0.38	1.85 ± 0.28
153	0.574 ± 0.031	0.425 ± 0.023	109	1.50 ± 0.23	1.11 ± 0.17
154-Sm	0.355 ± 0.005	0.263 ± 0.005	110	0.80 ± 0.12	0.59 ± 0.09
155-160	0.54 ± 0.14	0.40 ± 0.10	111	0.41 ± 0.06	0.30 ± 0.05
Σ	135.031 ± 1.026	100.004	112	0.20 ± 0.03	0.15 ± 0.02
			113-118	0.50 ± 0.12	0.37 ± 0.09

TABLE XVI

MEASURED ATOMS AND FAST FISSION YIELDS FOR ^{239}Pu - CAPSULE 24

HEAVY MASS PEAK			LIGHT MASS PEAK		
Mass No.	Atoms x10^{17}	Fission Yield	Mass No.	Atoms x10^{17}	Fission Yield
119-124	0.34 ± 0.09	0.28 ± 0.07	75-80	0.20 ± 0.05	0.17 ± 0.04
125-Sb	0.150 ± 0.017	0.13 ± 0.02	81	0.17 ± 0.02	0.14 ± 0.01
126	0.32 ± 0.05	0.27 ± 0.04	82	0.26 ± 0.02	0.22 ± 0.02
127	0.61 ± 0.09	0.51 ± 0.08	83-Kr	0.371 ± 0.003	0.310 ± 0.004
128	1.10 ± 0.14	0.92 ± 0.10	84-Kr	0.590 ± 0.005	0.492 ± 0.005
129	1.87 ± 0.20	1.56 ± 0.17	85Kr+Rb	0.724 ± 0.009	0.604 ± 0.008
130	3.00 ± 0.32	2.50 ± 0.26	86-Kr	0.933 ± 0.008	0.779 ± 0.009
131-Xe	4.557 ± 0.085	3.804 ± 0.064	87-Rb	1.261 ± 0.016	1.053 ± 0.016
132-Xe	6.246 ± 0.116	5.214 ± 0.100	88-Sr	1.601 ± 0.020	1.336 ± 0.019
133-Cs	8.438 ± 0.050	7.043 ± 0.062	89	2.026 ± 0.106	1.691 ± 0.090
134-Xe	8.788 ± 0.160	7.336 ± 0.107	90-Sr	2.452 ± 0.031	2.047 ± 0.027
135-Cs	9.137 ± 0.047	7.628 ± 0.064	91-Zr	3.032 ± 0.048	2.531 ± 0.044
136-Xe	8.317 ± 0.154	6.943 ± 0.100	92-Zr	3.684 ± 0.056	3.076 ± 0.052
137-Cs+Ba	7.992 ± 0.050	6.671 ± 0.060	93-Zr	4.642 ± 0.070	3.875 ± 0.065
138-Ba	7.412 ± 0.060	6.187 ± 0.065	94-Zr	5.220 ± 0.079	4.357 ± 0.073
139-La	6.736 ± 0.143	5.623 ± 0.120	95-Mo	5.735 ± 0.061	4.787 ± 0.062
140-Ce	6.394 ± 0.067	5.337 ± 0.077	96-Zr	5.909 ± 0.093	4.933 ± 0.085
141	6.094 ± 0.310	5.087 ± 0.247	97-Mo	6.486 ± 0.064	5.414 ± 0.067
142-Ce	5.794 ± 0.061	4.836 ± 0.055	98-Mo	6.896 ± 0.067	5.757 ± 0.071
143-Nd	5.294 ± 0.050	4.419 ± 0.048	99	7.467 ± 0.387	6.234 ± 0.326
144-Nd+Ce	4.496 ± 0.042	3.753 ± 0.038	100-Mo	8.041 ± 0.083	6.712 ± 0.085
145-Nd	3.642 ± 0.033	3.040 ± 0.032	101-Ru	7.828 ± 0.225	6.534 ± 0.145
146-Nd	2.985 ± 0.027	2.492 ± 0.026	102-Ru	7.982 ± 0.205	6.663 ± 0.125
147-Sm	2.419 ± 0.036	2.019 ± 0.032	103	7.925 ± 0.584	6.616 ± 0.478
148-Nd	2.003 ± 0.021	1.672 ± 0.020	104-Ru	7.869 ± 0.169	6.569 ± 0.106
149-Sm	1.494 ± 0.021	1.247 ± 0.019	105	6.511 ± 0.481	5.435 ± 0.394
150-Nd	1.190 ± 0.015	0.993 ± 0.014	106-Ru	5.152 ± 0.123	4.301 ± 0.083
151-Sm	0.947 ± 0.014	0.791 ± 0.014	107	3.60 ± 0.54	3.00 ± 0.45
152-Sm	0.717 ± 0.011	0.598 ± 0.010	108	2.20 ± 0.33	1.84 ± 0.28
153	0.519 ± 0.027	0.433 ± 0.023	109	1.30 ± 0.20	1.09 ± 0.17
154-Sm	0.320 ± 0.005	0.268 ± 0.005	110	0.72 ± 0.11	0.60 ± 0.09
155-160	0.48 ± 0.12	0.40 ± 0.10	111	0.36 ± 0.06	0.30 ± 0.05
			112	0.18 ± 0.03	0.15 ± 0.02
Σ	119.796 ± 0.889	100.004	113-118	0.47 ± 0.12	0.39 ± 0.10

TABLE XVII

MEASURED ATOMS AND FAST FISSION YIELDS FOR ^{239}Pu - CAPSULE 26

HEAVY MASS PEAK			LIGHT MASS PEAK		
Mass No.	Atoms $x10^{17}$	Fission Yield	Mass No.	Atoms $x10^{17}$	Fission Yield
119-124	0.38 ± 0.09	0.28 ± 0.07	75-80	0.23 ± 0.05	0.17 ± 0.04
125-Sb	0.173 ± 0.019	0.13 ± 0.02	81	0.19 ± 0.02	0.14 ± 0.01
126	0.37 ± 0.06	0.27 ± 0.04	82	0.30 ± 0.03	0.22 ± 0.02
127	0.73 ± 0.11	0.54 ± 0.08	83-Kr	0.426 ± 0.04	0.315 ±0.004
128	1.35 ± 0.17	1.00 ± 0.10	84-Kr	0.677 ± 0.006	0.502 ± 0.006
129	2.25 ± 0.23	1.67 ± 0.18	85-Kr+Rb	0.809 ± 0.009	0.599 ± 0.008
130	3.50 ± 0.37	2.59 ± 0.26	86-Kr	1.064 ± 0.009	0.789 ± 0.009
131-Xe	5.271 ± 0.093	3.907 ± 0.065	87-Rb	1.397 ± 0.017	1.035 ± 0.015
132-Xe	7.265 ± 0.135	5.385 ± 0.100	88-Sr	1.772 ± 0.022	1.313 ± 0.019
133-Cs	9.453 ± 0.056	7.007 ± 0.065	89	2.242 ± 0.117	1.662 ± 0.088
134-Xe	10.133 ± 0.185	7.511 ± 0.108	90-Sr	2.711 ± 0.036	2.010 ± 0.027
135-Cs	10.197 ± 0.052	7.558 ± 0.067	91-Zr	3.310 ± 0.085	2.454 ± 0.066
136-Xe	9.578 ± 0.177	7.099 ± 0.103	92-Zr	4.113 ± 0.108	3.049 ± 0.084
137-Cs+Ba	8.870 ± 0.055	6.574 ± 0.061	93-Zr	5.076 ± 0.133	3.763 ± 0.103
138-Ba	8.227 ± 0.066	6.098 ± 0.067	94-Zr	5.712 ± 0.144	4.234 ± 0.112
139-La	7.319 ± 0.368	5.425 ± 0.261	95-Mo	6.349 ± 0.071	4.706 ± 0.065
140-Ce	7.229 ± 0.077	5.358 ± 0.078	96-Zr	6.506 ± 0.166	4.822 ± 0.129
141	6.850 ± 0.360	5.077 ± 0.255	97-Mo	7.249 ± 0.071	5.373 ± 0.068
142-Ce	6.471 ± 0.069	4.796 ± 0.058	98-Mo	7.666 ± 0.075	5.682 ± 0.072
143-Nd	5.870 ± 0.056	4.351 ± 0.049	99	8.339 ± 0.434	6.181 ± 0.325
144-Nd+Ce	4.988 ± 0.047	3.697 ± 0.040	100-Mo	9.014 ± 0.095	6.681 ± 0.089
145-Nd	4.031 ± 0.036	2.988 ± 0.033	101-Ru	9.042 ± 0.266	6.702 ± 0.156
146-Nd	3.302 ± 0.030	2.448 ± 0.027	102-Ru	9.186 ± 0.238	6.809 ± 0.137
147-Sm	2.660 ± 0.039	1.972 ± 0.032	103	9.118 ± 0.677	6.758 ± 0.491
148-Nd	2.216 ± 0.023	1.643 ± 0.020	104-Ru	9.051 ± 0.214	6.709 ± 0.122
149-Sm	1.641 ± 0.023	1.216 ± 0.019	105	7.492 ± 0.558	5.553 ± 0.405
150-Nd	1.314 ± 0.016	0.974 ± 0.014	106-Ru	5.933 ± 0.227	4.397 ± 0.154
151-Sm	1.037 ± 0.015	0.769 ± 0.014	107	4.05 ± 0.61	3.00 ± 0.45
152-Sm	0.783 ± 0.011	0.581 ± 0.010	108	2.50 ± 0.37	1.85 ± 0.28
153	0.567 ± 0.030	0.420 ± 0.022	109	1.50 ± 0.23	1.11 ± 0.17
154-Sm	0.350 ± 0.005	0.259 ± 0.005	110	0.80 ± 0.12	0.59 ± 0.09
155-160	0.54 ± 0.14	0.40 ± 0.10	111	0.40 ± 0.06	0.30 ± 0.05
			112	0.20 ± 0.03	0.15 ± 0.02
Σ	134.915 ± 1.079	99.993	113-118	0.50 ± 0.12	0.37 ± 0.09

TABLE XVIII

SUMMARY ^{239}Pu FAST FISSION YIELDS

	HEAVY MASS PEAK					
	CAPSULE					
Mass No.	5	24	26	$\bar{X}$		σ
119-124	0.28	0.28	0.28	0.28	±	0.07
125-Sb	0.13	0.13	0.13	0.13	±	0.01
126	0.29	0.27	0.27	0.28	±	0.04
127	0.55	0.51	0.54	0.53	±	0.08
128	1.04	0.92	1.00	0.99	±	0.09
129	1.67	1.56	1.67	1.63	±	0.17
130	2.59	2.50	2.59	2.56	±	0.26
131-Xe	3.908	3.804	3.907	3.873	±	0.042
132-Xe	5.374	5.214	5.385	5.324	±	0.062
133-Cs	7.012	7.043	7.007	7.021	±	0.049
134-Xe	7.512	7.336	7.511	7.453	±	0.068
135-Cs	7.592	7.628	7.558	7.592	±	0.048
136-Xe	7.104	6.943	7.099	7.049	±	0.067
137-Cs+Ba	6.622	6.671	6.574	6.622	±	0.046
138-Ba	6.111	6.187	6.098	6.132	±	0.045
139-La	5.448	5.623	5.425	5.499	±	0.110
140-Ce	5.224	5.337	5.358	5.306	±	0.050
141	4.992	5.087	5.077	5.052	±	0.245
142-Ce	4.760	4.836	4.796	4.798	±	0.038
143-Nd	4.370	4.419	4.351	4.380	±	0.035
144-Nd+Ce	3.704	3.753	3.697	3.718	±	0.028
145-Nd	3.005	3.040	2.988	3.011	±	0.022
146-Nd	2.459	2.492	2.448	2.466	±	0.019
147-Sm	1.972	2.019	1.972	1.988	±	0.021
148-Nd	1.647	1.672	1.643	1.654	±	0.015
149-Sm	1.218	1.247	1.216	1.227	±	0.012
150-Nd	0.978	0.993	0.974	0.982	±	0.011
151-Sm	0.768	0.791	0.769	0.776	±	0.009
152-Sm	0.586	0.598	0.581	0.588	±	0.006
153	0.425	0.433	0.420	0.426	±	0.022
154-Sm	0.263	0.268	0.259	0.263	±	0.003
155-160	0.40	0.40	0.40	0.40	±	0.10
Spectral Index $^{238}U(n,f)/^{235}U(n,f)$	0.018	0.020	0.018	0.019		

TABLE XVIII (Cont'd)

SUMMARY ^{239}Pu FAST FISSION YIELDS

	LIGHT MASS PEAK					
	CAPSULE					
Mass No.	5	24	26	$\bar{X}$		σ
75-80	0.17	0.17	0.17	0.17	±	0.04
81	0.14	0.14	0.14	0.14	±	0.01
82	0.22	0.22	0.22	0.22	±	0.02
83-Kr	0.312	0.310	0.315	0.312	±	0.002
84-Kr	0.492	0.492	0.502	0.495	±	0.004
85-Kr+Rb	0.592	0.604	0.599	0.598	±	0.005
86-Kr	0.783	0.779	0.789	0.784	±	0.006
87-Rb	1.027	1.053	1.035	1.038	±	0.010
88-Sr	1.304	1.336	1.313	1.318	±	0.012
89	1.655	1.691	1.662	1.669	±	0.085
90-Sr	2.006	2.047	2.010	2.021	±	0.018
91-Zr	2.458	2.531	2.454	2.481	±	0.035
92-Zr	2.986	3.076	3.049	3.037	±	0.047
93-Zr	3.765	3.875	3.763	3.801	±	0.050
94-Zr	4.253	4.357	4.234	4.281	±	0.056
95-Mo	4.678	4.787	4.706	4.724	±	0.046
96-Zr	4.792	4.933	4.822	4.849	±	0.066
97-Mo	5.308	5.414	5.373	5.365	±	0.047
98-Mo	5.628	5.757	5.682	5.689	±	0.050
99	6.136	6.234	6.181	6.184	±	0.316
100-Mo	6.641	6.712	6.681	6.678	±	0.062
101-Ru	6.785	6.534	6.702	6.674	±	0.105
102-Ru	6.863	6.663	6.809	6.778	±	0.096
103	6.794	6.616	6.758	6.723	±	0.479
104-Ru	6.725	6.569	6.709	6.668	±	0.091
105	5.613	5.435	5.553	5.534	±	0.395
106-Ru	4.500	4.301	4.397	4.399	±	0.079
107	3.00	3.00	3.00	3.00	±	0.43
108	1.85	1.84	1.85	1.85	±	0.26
109	1.11	1.09	1.11	1.10	±	0.16
110	0.59	0.60	0.59	0.60	±	0.09
111	0.30	0.30	0.30	0.30	±	0.04
112	0.15	0.15	0.15	0.15	±	0.02
113-118	0.37	0.39	0.37	0.38	±	0.09

TABLE XIX

MEASURED ATOMS AND FAST FISSION YIELDS FOR ^{239}Pu - CAPSULE 35

HEAVY MASS PEAK			LIGHT MASS PEAK		
Mass No.	Atoms x10^{17}	Fission Yield	Mass No.	Atoms x10^{17}	Fission Yield
119-124	0.16 ± 0.04	0.28 ± 0.07	75-80	0.10 ± 0.02	0.17 ± 0.04
125-Sb	0.067 ± 0.007	0.12 ± 0.01	81	0.08 ± 0.01	0.14 ± 0.01
126	0.16 ± 0.02	0.28 ± 0.04	82	0.13 ± 0.01	0.22 ± 0.02
127	0.31 ± 0.05	0.53 ± 0.08	83-Kr	0.173 ± 0.001	0.298 ± 0.003
128	0.56 ± 0.07	0.96 ± 0.09	84-Kr	0.276 ± 0.002	0.476 ± 0.005
129	0.95 ± 0.10	1.64 ± 0.17	85-Kr+Rb	0.346 ± 0.004	0.596 ± 0.008
130	1.50 ± 0.16	2.59 ± 0.26	86-Kr	0.439 ± 0.004	0.757 ± 0.008
131-Xe	2.230 ± 0.041	3.843 ± 0.056	87-Rb	0.586 ± 0.007	1.010 ± 0.015
132-Xe	3.191 ± 0.058	5.500 ± 0.078	88-Sr	0.746 ± 0.009	1.286 ± 0.018
133-Cs	4.041 ± 0.024	6.965 ± 0.062	89	0.948 ± 0.005	1.634 ± 0.086
134-Xe	4.315 ± 0.078	7.437 ± 0.104	90-Sr	1.150 ± 0.014	1.983 ± 0.029
135-Cs	4.352 ± 0.022	7.502 ± 0.064	91-Zr	1.409 ± 0.023	2.428 ± 0.044
136-Xe	4.167 ± 0.075	7.182 ± 0.100	92-Zr	1.737 ± 0.028	2.995 ± 0.053
137-Cs+Ba	3.796 ± 0.024	6.544 ± 0.059	93-Zr	2.179 ± 0.034	3.756 ± 0.065
138-Ba	3.570 ± 0.029	6.154 ± 0.065	94-Zr	2.469 ± 0.039	4.255 ± 0.074
139-La	3.336 ± 0.071	5.750 ± 0.123	95-Mo	2.805 ± 0.030	4.836 ± 0.064
140-Ce	3.107 ± 0.032	5.355 ± 0.062	96-Zr	2.815 ± 0.045	4.853 ± 0.086
141	2.945 ± 0.153	5.076 ± 0.252	97-Mo	3.090 ± 0.031	5.327 ± 0.066
142-Ce	2.782 ± 0.029	4.796 ± 0.055	98-Mo	3.444 ± 0.033	5.937 ± 0.073
143-Nd	2.505 ± 0.024	4.319 ± 0.047	99	3.644 ± 0.189	6.282 ± 0.329
144-Nd+Ce	2.128 ± 0.020	3.667 ± 0.040	100-Mo	3.844 ± 0.040	6.626 ± 0.085
145-Nd	1.710 ± 0.015	2.948 ± 0.031	101-Ru	3.842 ± 0.109	6.623 ± 0.140
146-Nd	1.397 ± 0.013	2.408 ± 0.026	102-Ru	3.923 ± 0.083	6.762 ± 0.107
147-Sm	1.142 ± 0.016	1.969 ± 0.031	103	3.900 ± 0.287	6.722 ± 0.485
148-Nd	0.943 ± 0.010	1.625 ± 0.019	104-Ru	3.876 ± 0.083	6.682 ± 0.107
149-Sm	0.700 ± 0.010	1.206 ± 0.019	105	3.200 ± 0.237	5.516 ± 0.400
150-Nd	0.555 ± 0.007	0.957 ± 0.013	106-Ru	2.523 ± 0.058	4.349 ± 0.078
151-Sm	0.439 ± 0.006	0.756 ± 0.012	107	1.75 ± 0.26	3.02 ± 0.45
152-Sm	0.334 ± 0.005	0.576 ± 0.009	108	1.10 ± 0.17	1.90 ± 0.28
153	0.242 ± 0.013	0.416 ± 0.022	109	0.65 ± 0.10	1.12 ± 0.17
154-Sm	0.149 ± 0.002	0.257 ± 0.004	110	0.35 ± 0.05	0.60 ± 0.09
155-160	0.23 ± 0.06	0.40 ± 0.10	111	0.17 ± 0.02	0.29 ± 0.04
Σ	58.013 ± 0.438	100.008	112	0.09 ± 0.01	0.16 ± 0.02
			113-118	0.23 ± 0.06	0.40 ± 0.10

Spectral Index, $^{238}U(n,f)/^{235}U(n,f)$ 0.004

VI. ^{241}Pu FAST FISSION YIELDS

Two encapsulated samples of highly enriched ^{241}Pu oxide were irradiated and analyzed. The location of the samples in the irradiation assembly is shown in Figure 1. Both of these samples were irradiated in a softer spectrum (Table I) than the ^{239}Pu samples. In the treatment of the data, the results for both samples are pooled.

VI-A. ISOTOPIC COMPOSITION OF FISSION PRODUCT ELEMENTS

The isotopic composition of each fission product element measured is given in Tables XX through XXX. In all cases, except for krypton and xenon, the values are based on four individual unspiked analyses. For each of the listed isotopic abundances, the stated uncertainty is the standard deviation of the mean and only relates to the random error of the four measurements. The mean of the results for the two capsules and the associated standard deviation of the mean is tabulated.

Also included in these tables is the isotopic composition of the same fission product elements resulting from thermal neutron fission. The reference source is Walker's review[4]. The purpose of listing the isotopic results has been previously discussed (Section V-A).

VI-B. ABSOLUTE FISSION YIELDS

The number of atoms for each individual fission product nuclide obtained by measurement, interpolation, extrapolation, and estimation for each of the two capsules is given in Tables XXX and XXXII. Also given, for each capsule, is the total number of fissions based on the sum of the fission product atoms in the heavy mass peak, and the fission yield for each mass number.

In the following sections, many of the same comments apply as were presented for ^{239}Pu data and reference to those discussions is frequent.

VI-B-1. Heavy Mass Peak

VI-B-1-a. Mass Region 120-124. The number of atoms in the mass region 120-124 were estimated based on the measured value for ^{125}Sb and a comparison to the thermal yield data. Allowing for an increase in the yields of the valley nuclides, it is estimated that this portion of the heavy mass peak equals ∿0.17% of the total. A 25% relative error was assigned to this value.

VI-B-1-b. Mass 125. The atoms of mass 125 are based on a radiochemical measurement for ^{125}Sb.

VI-B-1-c. Mass Region 126-130. The same interpolation process used for the ^{239}Pu samples (Section V-B-1-c) was used for the ^{241}Pu samples. For ^{241}Pu fast fission, this region comprises ∿4.0% of the total atoms in the heavy mass peak. The uncertainty on the sum, ∿7.0% relative, was obtained by assuming a 10% relative error for each individual mass number estimate, and includes the error due to the uncertainty in the measured ^{125}Sb and xenon values.

VI-B-1-d. Xenon (Mass 131, 132, 134, 136). The measured isotopic composition of xenon is shown in Table XX. The $^{131}Xe/^{134}Xe$ ratio for fast fission is 4.5% greater than for thermal fission.

VI-B-1-e. Cesium (Mass 133, 135, 137). There is no significant difference between the isotopic composition of cesium (Table XXI) produced by fast fission and thermal fission for ^{241}Pu. A comparison of the number of mass 137 atoms determined from individual analyses of ^{137}Cs and ^{137}Ba gave similar results indicating no serious natural contamination problem (refer to Section V-B-1-e). In this compilation, the listed number of mass 137 atoms is the sum of the measured ^{137}Cs and ^{137}Ba atoms.

TABLE XX

ISOTOPIC COMPOSITION OF XENON
FROM ^{241}Pu FAST AND THERMAL FISSION

	FAST FISSION			
	CAPSULE			
Isotope	18	39	$\bar{X}/\sigma_{\bar{X}}$	Thermal[4] Fission
^{131}Xe	0.1404	0.1392	0.1398 ±0.0006	
^{132}Xe	0.2046	0.2036	0.2041 ±0.0005	
^{134}Xe	0.3459	0.3471	0.3465 ±0.0006	
^{136}Xe	0.3091	0.3100	0.3096 ±0.0005	
$^{131}Xe/^{134}Xe$	0.4059	0.4010	0.4035 ±0.0025	0.3860
$^{131}Xe/^{136}Xe$	0.4542	0.4490	0.4516 ±0.0013	
Renormalized to only include masses 131, 132, and 134.				
^{131}Xe	0.2032	0.2017	0.2024 ±0.0008	0.1968 ±0.0002
^{132}Xe	0.2961	0.2951	0.2956 ±0.0005	0.2933 ±0.0009
^{134}Xe	0.5007	0.5031	0.5019 ±0.0012	0.5099 ±0.0010

TABLE XXI

ISOTOPIC COMPOSITION OF CESIUM
FROM ^{241}Pu FAST AND THERMAL FISSION

	FAST FISSION			
	CAPSULE			
Isotope	18	39	$\bar{X}/\sigma_{\bar{X}}$	Thermal[4] Fission
^{133}Cs	0.3261 ±0.0001	0.3255 ±0.0001	0.3258 ±0.0003	
^{135}Cs	0.3555 ±0.0001	0.3559 ±0.0001	0.3557 ±0.0002	
^{137}Cs	0.3184 ±0.0001	0.3186 ±0.0001	0.3185 ±0.0001	
$^{133}Cs/^{137}Cs$	1.024	1.022	1.023 ±0.001	1.023
Renormalized to only include masses 133 and 137.				
^{133}Cs	0.5060 ±0.0001	0.5054 ±0.0001	0.5057 ±0.0003	0.5056 ±0.0086
^{137}Cs	0.4940 ±0.0001	0.4946 ±0.0001	0.4943 ±0.0003	0.4944 ±0.0084

VI-B-1-f. Barium (Mass 138). The atoms of mass 138 were determined from an analysis of barium. The method used to validate the absence of serious natural contamination problems has been previously discussed (Section V-B-1-f).

VI-B-1-g. Lanthanum (Mass 139). For reasons previously given (Section V-B-1-g), the error associated with the measured number of ^{139}La atoms is greater than for other isotopes.

VI-B-1-h. Cerium (Mass 140, 142). The isotopic abundances for ^{140}Ce and ^{142}Ce for fast and thermal ^{241}Pu fission are given in Table XXII. Comments relative to improved mass spectrometric measurement techniques for cerium are given in Section V-B-1-h. The reason for the nearly 7% difference in the $^{140}Ce/^{142}Ce$ ratio for fast and thermal fission is not known.

TABLE XXII

ISOTOPIC COMPOSITION OF CERIUM
FROM ^{241}Pu FAST AND THERMAL FISSION

	FAST FISSION			
	CAPSULE			
Isotope	18	39	$\bar{X}/\sigma_{\bar{X}}$	Thermal[4] Fission
^{140}Ce	0.5339 ±0.0019	0.5363 ±0.0008	0.5351 ±0.0012	0.5515 ±0.0011
^{142}Cs	0.4661 ±0.0019	0.4637 ±0.0008	0.4649 ±0.0012	0.4485 ±0.0005
$^{140}Ce/^{142}Ce$	1.145	1.157	1.151 ±0.006	1.230

VI-B-1-i. Mass 141. The atoms of mass 141 were obtained by linear interpolation between the measured atoms of ^{140}Ce and ^{142}Ce. The number of mass 141 atoms comprises ∿5.0% of the total heavy mass peak. The propagated relative uncertainty is 5.2% which includes an assigned 5% relative systematic error and the error due to the uncertainty in the measured atoms of cerium.

VI-B-1-j. Neodymium (Mass 143, 144, 145, 146, 148, 150). The measured isotopic composition of neodymium for fast and thermal fission is given in Table XXIII.

These data show only a small change in the $^{150}Nd/^{143}Nd$ isotopic ratio compared to ^{239}Pu and especially ^{235}U. This decrease is attributed to a slight shift in the heavy mass peak to a larger average mass, thus rendering the isotopic composition of the 143-150 mass region less sensitive to change in neutron energy.

TABLE XXIII

ISOTOPIC COMPOSITION OF NEODYMIUM
FROM ^{241}Pu FAST AND THERMAL FISSION

	FAST FISSION			
	CAPSULE			
Isotope	18	39	$\bar{X}/\sigma_{\bar{X}}$	Thermal[4] Fission
^{143}Nd	0.2568 ±0.0001	0.2567 ±0.0001	0.2568 ±0.0001	0.2551 ±0.0013
^{144}Nd	0.2346 ±0.0001	0.2347 ±0.0001	0.2346 ±0.0001	0.2356 ±0.0028
^{145}Nd	0.1827 ±0.0001	0.1828 ±0.0001	0.1828 ±0.0001	0.1814 ±0.0007
^{146}Nd	0.1527 ±0.0001	0.1529 ±0.0001	0.1528 ±0.0001	0.1532 ±0.0014
^{148}Nd	0.1066 ±0.0001	0.1065 ±0.0001	0.1066 ±0.0001	0.1082 ±0.0011
^{150}Nd	0.0665 ±0.0001	0.0664 ±0.0001	0.0664 ±0.0001	0.0663 ±0.0020
$^{150}Nd/^{143}Nd$	0.2590	0.2587	0.2588 ±0.0002	0.2599

VI-B-1-k. Samarium (Mass 147, 149, 151, 152, 154). The isotopic composition of samarium for fast and thermal fission is given in Table XXIV. Similar to the ^{239}Pu data, comparison of fast and thermal data is difficult because of the numerous neutron capture corrections which are applied to the thermal data.[4] The value for ^{147}Sm was corrected for decay of ^{147}Pm using a half-life of 2.623y. For ^{151}Sm, a half-life of 93y was used.

TABLE XXIV

ISOTOPIC COMPOSITION OF SAMARIUM
FROM ^{241}Pu FAST AND THERMAL FISSION

	FAST FISSION			
	CAPSULE			
Isotope	18	39	$\bar{X}/\sigma_{\bar{X}}$	Thermal Fission
^{147}Sm	0.3947 ±0.0003	0.3937 ±0.0003	0.3942 ±0.0005	0.3936 ±0.0024
^{149}Sm	0.2564 ±0.0004	0.2557 ±0.0001	0.2560 ±0.0004	0.2565 ±0.0018
^{151}Sm	0.1603 ±0.0004	0.1611 ±0.0002	0.1607 ±0.0004	0.1577 ±0.0016
^{152}Sm	0.1241 ±0.0003	0.1240 ±0.0002	0.1240 ±0.0001	0.1245 ±0.0012
^{154}Sm	0.0645 ±0.0004	0.0654 ±0.0002	0.0650 ±0.0005	0.0676 ±0.0006
$^{147}Sm/^{154}Sm$	6.119	6.020	6.070 ±0.050	5.822
$^{147}Sm/^{152}Sm$	3.180	3.175	3.178 ±0.003	3.161

VI-B-1-ℓ. Mass 153. The atoms of mass 153 were obtained by linear interpolation between the measured atoms of ^{152}Sm and ^{154}Sm. Mass 153 comprises ∿0.54% of the heavy mass peak. The propagated relative uncertainty is 5.2%, which includes an assigned 5% relative systematic error for mass 153 and the error due to the uncertainty in the measured atoms of samarium.

VI-B-1-m. Mass Region 156-160. The number of atoms in this mass region was obtained by extrapolating the measured number of atoms in the 150-154 mass region to mass 160. The mass region 155-160 constitutes ∿0.7% of the heavy mass peak, to which a 25% relative uncertainty has been assigned.

VI-B-2. Light Mass Peak

VI-B-2-a. Mass Region 75-82. The number of atoms in the mass region 75 through 82 was obtained by extrapolating the measured number of atoms of the krypton isotopes to mass 75. The region from mass 75-80 is listed as an individual value, and mass 81 and 82 are listed as separate values.

VI-B-2-b. Krypton (Mass 83, 84, 86). Table XXV gives the isotopic composition of krypton produced by fast and thermal fission of ^{241}Pu. As in the case of ^{239}Pu, the $^{86}Kr/^{83}Kr$ ratio is smaller for fast fission than for thermal fission corresponding to a broadening of the wings of the mass yield curve with increasing neutron energy. The value for ^{85}Kr is included with the rubidium data in Table XXVI.

TABLE XXV

ISOTOPIC COMPOSITION OF KRYPTON
FROM ^{241}Pu FAST AND THERMAL FISSION

	FAST FISSION			
	CAPSULE			
Isotope	18	39	$\bar{X}/\sigma_{\bar{X}}$	Thermal[4] Fission
^{83}Kr	0.1749	0.1755	0.1752 ±0.0003	0.1727 ±0.0002
^{84}Kr	0.3084	0.3073	0.3078 ±0.0006	0.3075 ±0.0010
^{86}Kr	0.5167	0.5171	0.5169 ±0.0002	0.5198 ±0.0005
$^{86}Kr/^{83}Kr$	2.954	2.946	2.950 ±0.004	3.010

VI-B-2-c. Rubidium (Mass 85, 87). The isotopic composition of rubidium resulting from fast and thermal ^{241}Pu fission is given in Table XXVI. The abundance of mass 85 was obtained by summing the measured atoms of ^{85}Kr and ^{85}Rb.

TABLE XXVI

ISOTOPIC COMPOSITION OF RUBIDIUM
FROM ^{241}Pu FAST AND THERMAL FISSION

	FAST FISSION			
	CAPSULE			
Isotope	18	39	$\bar{X}/\sigma_{\bar{X}}$	Thermal[4] Fission
$^{85}Kr+^{85}Rb$	0.3455	0.3456	0.3456 ±0.0001	0.3434 ±0.0003
^{87}Rb	0.6545	0.6544	0.6544 ±0.0001	0.6566 ±0.0007
$^{85}Rb/^{87}Rb$	0.5279	0.5281	0.5280 ±0.0001	0.5230

VI-B-2-d. Strontium (Mass 88, 90). Table XXVII gives the isotopic composition of strontium produced by fast and thermal ^{241}Pu fission. The value for mass 90 was obtained by summing the measured atoms of ^{90}Sr and ^{90}Zr.

TABLE XXVII

ISOTOPIC COMPOSITION OF STRONTIUM
FROM ^{241}Pu FAST AND THERMAL FISSION

	FAST FISSION			
	CAPSULE			
Isotope	18	39	$\bar{X}/\sigma_{\bar{X}}$	Thermal[4] Fission
^{88}Sr	0.3859	0.3870	0.3864 ±0.0006	0.3845 ±0.0012
^{90}Sr	0.6141	0.6130	6.6136 ±0.0006	0.6155 ±0.0012
$^{88}Sr/^{90}Sr$	0.6284	0.6313	0.6299 ±0.0015	0.6247

VI-B-2-e. Mass 89. The atoms of mass 89 were obtained by linear extrapolation between the measured atoms of ^{88}Sr and ^{90}Sr. The propagated uncertainty associated with this value is 5.2% relative, which includes an assigned 5% relative systematic error, and the error due to the uncertainty in the measured strontium atoms.

VI-B-2-f. Zirconium (Mass 91, 92, 93, 94, 96). The isotopic composition of zirconium produced by fast and thermal fission of ^{241}Pu is given in Table XXVIII. Comments relative to the natural contamination given in Section V-B-2-f for ^{239}Pu data also apply to ^{241}Pu.

TABLE XXVIII

ISOTOPIC COMPOSITION OF ZIRCONIUM
FROM ^{241}Pu FAST AND THERMAL FISSION

	FAST FISSION			
	CAPSULE			
Isotope	18	39	$\bar{X}/\sigma_{\bar{X}}$	Thermal[4] Fission
^{91}Zr	0.1275 ±0.0008	0.1253 ±0.0002	0.1264 ±0.0011	0.1245 ±0.0001
^{92}Zr	0.1552 ±0.0007	0.1566 ±0.0002	0.1559 ±0.0007	0.1526 ±0.0005
^{93}Zr	0.1993 ±0.0009	0.1969 ±0.0001	0.1981 ±0.0012	0.1984 ±0.0004
^{94}Zr	0.2270 ±0.0005	0.2277 ±0.0003	0.2274 ±0.0004	0.2280 ±0.0004
^{96}Zr	0.2910 ±0.0009	0.2935 ±0.0002	0.2922 ±0.0013	0.2965 ±0.0003
^{91}Zr/^{96}Zr	0.4381	0.4269	0.4325 ±0.0056	0.4199

VI-B-2-g. Molybdenum (Mass 95, 97, 98, 100). The isotopic composition of molybdenum for ^{241}Pu fast fission is given in Table XXIX. As noted in the table, no mass spectrometric data exist for ^{241}Pu thermal fission. The quoted values are from the ENDF-B/V-C unpublished compilation and are based on radiochemical measurements.

VI-B-2-h. Mass 99. The atoms of mass 99 were determined by linear interpolation between the measured atoms of ^{98}Mo and ^{100}Mo. The propagated uncertainty associated with this value is 5.2% relative, which includes an assigned systematic error of 5% relative and the error due to the uncertainty in the measured molybdenum atoms.

TABLE XXIX

ISOTOPIC COMPOSITION OF MOLYBDENUM
FROM ^{241}Pu FAST AND THERMAL FISSION

	FAST FISSION			
	CAPSULE			
Isotope	18	39	$\bar{X}/\sigma_{\bar{X}}$	Thermal[a] Fission
^{95}Mo	0.1980	0.1978	0.1979 ±0.0001	0.2012
^{97}Mo	0.2351	0.2347	0.2349 ±0.0002	0.2385
^{98}Mo	0.2506	0.2507	0.2506 ±0.0001	0.2556
^{100}Mo	0.3163	0.3168	0.3166 ±0.0003	0.3047
$^{95}Mo/^{100}Mo$	0.6260	0.6244	0.6252 ±0.0008	0.6603

[a] No measurements reported for the isotopic composition of fission product Mo for ^{241}Pu thermal fission. The listed values were obtained from ENDF-B/V-C (Unpublished March 1977).

VI-B-2-i. Ruthenium (Mass 101, 102, 103, 104, 105, 106). The measured isotopic composition of ruthenium for mass numbers 101, 102, 104, and 106 for fast and thermal ^{241}Pu fission is given in Table XXX. In Section V-B-2-i, the problem of ruthenium plate-out in the dissolution of the ^{239}Pu was discussed. For the two ^{241}Pu capsule, one (No. 18) showed a 13.4% loss of ruthenium during dissolution, and the other (No. 39) showed <1% loss. That little or no ruthenium had plated out in this latter case was confirmed by the absence of detectable ^{106}Ru on the dissolution equipment and the filter through which the dissolver solution was passed. For this case, the actual measured number of ruthenium atoms was used to calculate the fission yields. For capsule 18, the same correction procedure previously described (Section V-B-2-i) was used.

TABLE XXX

ISOTOPIC COMPOSITION OF RUTHENIUM
FROM ^{241}Pu FAST AND THERMAL FISSION

	FAST FISSION			
	CAPSULE			
Isotope	18	39	$\overline{X}/\sigma_{\overline{X}}$	Thermal[4] Fission
^{101}Ru	0.2412 ±0.0004	0.2409 ±0.0004	0.2410 ±0.0002	0.2363
^{102}Ru	0.2544 ±0.0004	0.2559 ±0.0003	0.2552 ±0.0007	0.2514
^{104}Ru	0.2714 ±0.0007	0.2719 ±0.0003	0.2716 ±0.0003	0.2705
^{106}Ru	0.2330 ±0.0012	0.2313 ±0.0026	0.2321 ±0.0009	0.2418
$^{101}Ru/^{106}Ru$	1.035	0.042	1.038 ±0.004	0.9773

VI-B-2-j. Mass Region 107-112. The number of atoms for each of these mass numbers was obtained by extrapolating the mass yield curve from the ruthenium region toward the valley region. Thermal yield data were used as a guide. Unfortunately, no ^{241}Pu energy dependent yield data for mass 111 are available for use as a reference point (refer to Section V-B-2-j and k). The assigned error associated with each mass number is 25% relative.

VI-B-2-ℓ. Mass 113-119. The number of atoms in this mass region was obtained by estimation, attempting to account for the increase in the abundance of the valley nuclides with increasing neutron energy. A 25% relative uncertainty was assigned to this value.

VI-C. ERROR ANALYSIS

The same error analysis treatment described for the ^{239}Pu data (Section V-C) applies to the ^{241}Pu data.

TABLE XXXI

MEASURED ATOMS AND FAST FISSION YIELDS FOR ^{241}Pu - CAPSULE 18

HEAVY MASS PEAK			LIGHT MASS PEAK		
Mass No.	Atoms x10^{17}	Fission Yield	Mass No.	Atoms x10^{17}	Fission Yield
120-124	0.15±0.04	0.17±0.04	75-80	0.12±0.03	0.13±0.03
125-Sb	0.059±0.007	0.066±0.007	81	0.08±0.01	0.09±0.01
126	0.14±0.02	0.16±0.02	82	0.12±0.01	0.13±0.01
127	0.29±0.04	0.33±0.05	83-Kr	0.178±0.002	0.200±0.003
128	0.56±0.07	0.63±0.06	84-Kr	0.313±0.003	0.352±0.004
129	0.98±0.10	1.10±0.11	85-Kr+Rb	0.354±0.002	0.398±0.003
130	1.60±0.17	1.80±0.18	86-Kr	0.525±0.006	0.590±0.007
131-Xe	2.787±0.036	3.133±0.035	87-Rb	0.671±0.002	0.754±0.005
132-Xe	4.062±0.050	4.567±0.048	88-Sr	0.858±0.004	0.965±0.007
133-Cs	5.975±0.034	6.718±0.051	89	1.112±0.057	1.250±0.064
134-Xe	6.864±0.082	7.718±0.079	90-Sr+Zr	1.366±0.077	1.536±0.011
135-Cs	6.513±0.032	7.324±0.051	91-Zr	1.693±0.024	1.903±0.029
136-Xe	6.133±0.076	6.896±0.073	92-Zr	2.061±0.027	2.318±0.033
137-Cs+Ba	5.834±0.033	6.560±0.047	93-Zr	2.647±0.034	2.976±0.042
138-Ba	5.715±0.034	6.426±0.052	94-Zr	3.015±0.037	3.390±0.046
139-La	5.628±0.159	6.328±0.171	95-Mo	3.495±0.022	3.929±0.034
140-Ce	4.809±0.057	5.408±0.063	96-Zr	3.865±0.050	4.456±0.061
141	4.504±0.235	5.064±0.251	97-Mo	4.150±0.021	4.667±0.037
142-Ce	4.198±0.057	4.720±0.056	98-Mo	4.424±0.020	4.974±0.037
143-Nd	4.109±0.031	4.620±0.040	99	5.004±0.255	5.626±0.288
144-Nd+Ce	3.753±0.026	4.221±0.034	100-Mo	5.583±0.031	6.278±0.051
145-Nd	2.924±0.020	3.288±0.026	101-Ru	5.655±0.077	6.359±0.059
146-Nd	2.443±0.017	2.747±0.022	102-Ru	5.963±0.080	6.705±0.062
147-Sm	1.985±0.015	2.232±0.020	103	6.163±0.444	6.930±0.494
148-Nd	1.705±0.014	1.917±0.018	104-Ru	6.362±0.087	7.154±0.067
149-Sm	1.289±0.009	1.450±0.013	105	5.913±0.425	6.649±0.473
150-Nd	1.065±0.011	1.197±0.013	106-Ru	5.462±0.081	6.142±0.068
151-Sm	0.806±0.006	0.907±0.008	107	4.50±1.13	5.06±1.27
152-Sm	0.624±0.005	0.702±0.007	108	3.00±0.75	3.37±0.84
153	0.474±0.025	0.533±0.028	109	2.00±0.50	2.25±0.56
154-Sm	0.325±0.004	0.365±0.005	110	1.20±0.30	1.35±0.34
155-160	0.63 ±0.16	0.71 ±0.18	111	0.50±0.13	0.56±0.14
			112	0.25±0.06	0.28±0.07
Σ	88.933±0.527	100.007	113-119	0.34±0.09	0.38±0.09

TABLE XXXII

MEASURED ATOMS AND FAST FISSION YIELDS FOR ^{241}Pu - CAPSULE 39

HEAVY MASS PEAK			LIGHT MASS PEAK		
Mass No.	Atoms x10^{17}	Fission Yield	Mass No.	Atoms x10^{17}	Fission Yield
120-124	0.14±0.03	0.16±0.04	75-80	0.11±0.03	0.13±0.03
125-Sb	0.043±0.005	0.049±0.005	81	0.08±0.01	0.09±0.01
126	0.12±0.02	0.14±0.02	82	0.12±0.01	0.14±0.01
127	0.27±0.04	0.31±0.05	83-Kr	0.172±0.002	0.197±0.002
128	0.56±0.07	0.64±0.06	84-Kr	0.301±0.003	0.346±0.004
129	0.98±0.10	1.13±0.12	85-Kr+Rb	0.347±0.003	0.398±0.003
130	1.60±0.16	1.84±0.19	86-Kr	0.506±0.005	0.582±0.007
131-Xe	2.751±0.035	3.160±0.035	87-Rb	0.656±0.004	0.754±0.006
132-Xe	4.023±0.050	4.621±0.049	88-Sr	0.844±0.005	0.969±0.008
133-Cs	5.875±0.034	6.748±0.051	89	1.091±0.056	1.253±0.065
134-Xe	6.859±0.082	7.878±0.080	90-Sr+Zr	1.337±0.009	1.535±0.011
135-Cs	6.423±0.031	7.377±0.052	91-Zr	1.657±0.021	1.903±0.027
136-Xe	6.126±0.076	7.036±0.075	92-Zr	2.070±0.025	2.377±0.032
137-Cs+Ba	5.751±0.032	6.605±0.047	93-Zr	2.603±0.031	2.990±0.040
138-Ba	5.620±0.021	6.455±0.044	94-Zr	3.011±0.036	3.458±0.046
139-La	5.302±0.150	6.090±0.165	95-Mo	3.421±0.022	3.929±0.034
140-Ce	4.657±0.055	5.349±0.062	96-Zr	3.880±0.048	4.345±0.061
141	4.342±0.227	4.987±0.247	97-Mo	4.059±0.019	4.662±0.035
142-Ce	4.027±0.048	4.626±0.054	98-Mo	4.335±0.017	4.979±0.036
143-Nd	3.987±0.030	4.579±0.039	99	4.908±0.348	5.637±0.401
144-Nd+Ce	3.625±0.025	4.185±0.034	100-Mo	5.480±0.031	6.295±0.051
145-Nd	2.839±0.019	3.260±0.026	101-Ru	5.525±0.033	6.345±0.053
146-Nd	2.375±0.016	2.728±0.022	102-Ru	5.867±0.034	6.739±0.056
147-Sm	1.956±0.014	2.247±0.020	103	6.051±0.429	6.949±0.494
148-Nd	1.653±0.014	1.899±0.018	104-Ru	6.234±0.036	7.160±0.059
149-Sm	1.270±0.009	1.459±0.013	105	5.769±0.409	6.626±0.471
150-Nd	1.032±0.011	1.186±0.013	106-Ru	5.304±0.067	6.092±0.085
151-Sm	0.801±0.006	0.920±0.008	107	4.40±1.10	5.05±1.26
152-Sm	0.616±0.005	0.708±0.007	108	2.90±0.73	3.33±0.83
153	0.471±0.024	0.541±0.028	109	1.90±0.48	2.18±0.55
154-Sm	0.325±0.003	0.374±0.004	110	1.20±0.30	1.38±0.34
155-160	0.63 ±0.16	0.72 ±0.18	111	0.50±0.13	0.57±0.14
			112	0.25±0.06	0.29±0.07
Σ	87.049±0.515	100.007	113-119	0.33±0.08	0.38±0.09

TABLE XXXIII

SUMMARY ^{241}Pu FAST FISSION YIELDS

	HEAVY MASS PEAK			
	CAPSULE			
Mass No.	18	39	$\bar{X}$	σ
120-124	0.17	0.16	0.17 ±	0.04
125-Sb	0.066	0.049	0.058 ±	0.009
126	0.16	0.14	0.15 ±	0.02
127	0.33	0.31	0.32 ±	0.05
128	0.63	0.64	0.64 ±	0.06
129	1.10	1.13	1.12 ±	0.11
130	1.80	1.84	1.82 ±	0.18
131-Xe	3.133	3.160	3.147 ±	0.028
132-Xe	4.567	4.621	4.594 ±	0.038
133-Cs	6.718	6.748	6.733 ±	0.043
134-Xe	7.718	7.878	7.798 ±	0.086
135-Cs	7.324	7.377	7.351 ±	0.043
136-Xe	6.896	7.036	6.966 ±	0.079
137-Cs+Ba	6.560	6.605	6.583 ±	0.041
138-Ba	6.426	6.455	6.441 ±	0.040
139-La	6.328	6.090	6.209 ±	0.124
140-Ce	5.408	5.349	5.379 ±	0.048
141	5.064	4.987	5.026 ±	0.244
142-Ce	4.720	4.626	4.673 ±	0.053
143-Nd	4.620	4.579	4.600 ±	0.033
144-Nd+Ce	4.221	4.185	4.203 ±	0.028
145-Nd	3.288	3.260	3.274 ±	0.021
146-Nd	2.747	2.728	2.738 ±	0.018
147-Sm	2.232	2.247	2.240 ±	0.017
148-Nd	1.917	1.899	1.908 ±	0.015
149-Sm	1.450	1.459	1.455 ±	0.010
150-Nd	1.197	1.186	1.192 ±	0.012
151-Sm	0.907	0.920	0.914 ±	0.007
152-Sm	0.702	0.708	0.705 ±	0.006
153	0.533	0.541	0.537 ±	0.027
154-Sm	0.365	0.374	0.370 ±	0.005
155-160	0.71	0.72	0.72 ±	0.18
Spectral Index $^{238}U(n,f)/^{235}U(n,f)$	~0.007	0.004		

TABLE XXXIII (Cont'd)

SUMMARY ^{241}Pu FAST FISSION YIELDS

	LIGHT MASS PEAK				
	CAPSULE				
Mass No.	18	39	$\bar{X}$		σ
75-80	0.13	0.13	0.13	±	0.03
81	0.09	0.09	0.09	±	0.01
82	0.13	0.14	0.14	±	0.01
83-Kr	0.200	0.197	0.199	±	0.002
84-Kr	0.352	0.346	0.349	±	0.003
85-Kr+Rb	0.398	0.398	0.398	±	0.003
86-Kr	0.590	0.582	0.586	±	0.005
87-Rb	0.754	0.754	0.754	±	0.005
88-Sr	0.965	0.969	0.967	±	0.006
89	1.250	1.253	1.252	±	0.064
90-Sr	1.536	1.535	1.536	±	0.009
91-Zr	1.903	1.903	1.903	±	0.021
92-Zr	2.318	2.377	2.348	±	0.032
93-Zr	2.976	2.990	2.983	±	0.031
94-Zr	3.390	3.458	3.424	±	0.034
95-Mo	3.929	3.929	3.929	±	0.030
96-Zr	4.456	4.345	4.401	±	0.061
97-Mo	4.667	4.662	4.665	±	0.031
98-Mo	4.974	4.979	4.977	±	0.032
99	5.626	5.637	5.632	±	0.342
100-Mo	6.278	6.295	6.287	±	0.046
101-Ru	6.359	6.345	6.352	±	0.041
102-Ru	6.705	6.739	6.722	±	0.043
103	6.930	6.949	6.940	±	0.351
104-Ru	7.154	7.160	7.157	±	0.046
105	6.649	6.626	6.638	±	0.335
106-Ru	6.142	6.092	6.117	±	0.056
107	5.06	5.05	5.06	±	0.90
108	3.37	3.33	3.35	±	0.59
109	2.25	2.18	2.22	±	0.39
110	1.35	1.38	1.37	±	0.10
111	0.56	0.57	0.57	±	0.10
112	0.28	0.29	0.29	±	0.05
113-119	0.38	0.38	0.38	±	0.09

VII. BURNUP MONITORS

Based on the augmented ^{239}Pu fission yield data given in this report, and discussions previously presented[2] regarding the selection of fission monitors for the determination of burnup in FBR fuels, the following recommendation is made:

> For mixed-oxide fuels where the major sources of fission are ^{235}U and ^{239}Pu and the neutron spectrum is characteristic of a mixed-oxide fueled LMFBR, the preferred monitor is ^{148}Nd and the recommended fission yield is 1.66%.

The additional ^{239}Pu fission yield data presented in this report have not altered our previous position relative to this recommendation.

For oxide fuels irradiated in a neutron spectrum characteristic of an oxide fueled LMFBR, where the major sources of fission are from ^{239}Pu and ^{241}Pu, it is suggested that the use of ^{143}Nd be considered as the fission monitor. Although this is only in the form of a suggestion, it is based on the fact that there is less difference ($\sim$5%) between the ^{143}Nd fast fission yields for ^{239}Pu and ^{241}Pu than for the other isotopes of neodymium. The final recommendation will depend upon the fission yield values obtained for ^{240}Pu and ^{242}Pu fast fission.

REFERENCES

1. W. J. Maeck, R. P. Larsen, J. E. Rein, "Burnup Determination for Fast Reactor Fuels: A Review of the Status of Nuclear Data and Analytical Chemistry Methodology Requirements", USERDA Rept., TID-26209 (1973).

2. W. J. Maeck, Ed., "Fast Reactor Fission Yields for ^{233}U, ^{235}U, ^{238}U, ^{239}Pu, and Recommendations for the Determination of Burnup on FBR Mixed-Oxide Fuels: An Interim Project Report", Allied Chemical Corporation - Idaho Chemical Programs, Rept., ICP-1050-I (1973).

3. J. A. Hallbid, Sandia Corporation Rept., SC-RR-70-251 (1970).

4. W. H. Walker, "Fission Product Data for Thermal Reactors, Part II - Yields", Atomic Energy of Canada Limited Rept., AECL-3037, Part II (1973).

5. W. J. Maeck, W. A. Emel, J. E. Delmore, F. A. Duce, L. L. Dickerson, J. H. Keller, R. L. Tromp, "Discrepancies and Comments Regarding ^{235}U and ^{239}Pu Thermal Fission Yields and the Use of ^{148}Nd as a Burnup Monitor", Allied Chemical Corporation - Idaho Chemical Programs Rept., ICP-1092 (1976).

6. W. J. Maeck, Review Paper No. 5, IAEA-169 Panel on Fission Product Nuclear Data, Bologna, Italy (1973).

7. J. C. Cunninghame, H. H. Willis, J. Inorg. Nucl. Chem., 39, (1977).

APPENDIX

The chemical separation procedures used in this work were developed to require a minimum number of manipulations and minimal use of reagents to maintain as low as practical levels of natural contamination. All mineral acids were quartz distilled and special reagents were purified before use. Whenever possible, plastic-ware was used in the chemical separation procedures. All dissolution, and chemical separation glass- and plastic-ware, were discarded after a single use.

Three mass spectrometers were used in the analysis program. For krypton and xenon, the data were obtained using a Hitachi Model RMU-6E gas mass spectrometer with a Faraday Cage collector and vibrating reed electrometer. Two thermal ionization mass spectrometers were used for the solid fission products. One is a single stage, 60 degree magnetic sector mass spectrometer equipped with both a deep Faraday Cage collector and a 20-stage ion multiplier. The other is a tandem 90-degree sector mass spectrometer equipped with a pulse counting system. The single stage instrument was primarily used for the analysis of those elements which have high sensitivity and which do not require the measurement of large isotopic ratios (i.e., Rb, Cs, Ba, Sr, Nd, and Sm). For those elements which have less than desirable sensitivity (i.e., Zr, Mo, Ru), or where the measurement of very large isotopic ratios is required (i.e., La, Ce), the tandem mass spectrometer was used. Because of its high sensitivity, the tandem mass spectrometer was also used if the quantity of the sample being measured was low.

All sample and ionizing filaments were pre-baked before using, because it is next to impossible to obtain 100% pure filament material. The most difficult materials to remove are zirconium and molybdenum. These elements can interfere in the analysis of zirconium, molybdenum, and ruthenium, especially if a high filament temperature is required to obtain a suitable analysis. To minimize this interference problem, a rigid quality control program was instigated and constant surveillance of the spectra was required to determine that no interference was occurring from the contaminants in the filament material during

the course of the measurements.

A-1. Rubidium, Cesium, Strontium, and Barium

Chemical separation - These elements, which have similar chemical properties, are sequentially separated from a single sample aliquot.

For the concentration measurement, a weighed aliquot of the dissolved sample solution is added to weighed aliquots of enriched ^{85}Rb, ^{133}Cs, ^{87}Sr, and ^{135}Ba spikes, and the mixture is evaporated to near dryness. The residue is dissolved in H_2O and the hydrolyzable ions are sequentially removed by precipitation with NH_4OH and then by passing the solution through a OH^- form anion column. The column effluent is evaporated to dryness. The residue is dissolved in a minimum amount of 0.5M HNO_3, and the solution is loaded on a H^+ form cation column. The rubidium and cesium fractions are eluted with 1.0M HNO_3 and collected together. The strontium and barium fractions are chromatographically eluted with 2.0M HNO_3, and collected separately.

Mass spectrometry - Rubidium and cesium which have nearly identical ionization properties in the mass spectrometer, and do not interfere with one another, are mounted on the same mass spectrometer filament and sequentially analyzed. In this case, the dried mixed rubidium-cesium sample is dissolved in ~0.01 mL 1M HCl and loaded onto a prebaked Ta side filament and dried. A prebaked Re center filament serves as the ionizing filament. Rubidium is analyzed first because it is more sensitive to fractionation as a function of time than is cesium.

Although chemically similar, the ionization characteristics of strontium and barium are sufficiently different that superior results are obtained if each element is mounted and analyzed separately rather than using the multiple analysis technique. The same sample loading procedure and filament material described above are used for individual barium and strontium fractions. Because cesium can interfere with barium, and rubidium with strontium, the presence of the alkali metals must be monitored prior to and during the collection of the barium and strontium data.

A-2. Lanthanum, Cerium, Neodymium, and Samarium

Chemical separation - These lanthanide elements are first separated as a group and then chromatographically separated into individual fractions. For concentration measurements, a weighed aliquot of the dissolved sample solution is added to weighed aliquots of enriched ^{138}La, ^{136}Ce, ^{150}Nd, and ^{144}Sm spikes and mixed. The lanthanides are precipitated as the hydroxides using NH_4OH, dissolved in HCl and reprecipitated with a minimum amount of NH_4OH. After washing, the precipitate is dissolved in 10M HCl, the solution loaded on a Cl^- form anion column, and the lanthanides are eluted with 10M HCl separating them from the bulk of the plutonium.

The lanthanides are separated from the 10M HCl solution by precipitation using NaOH and nickel carrier. The precipitate is dissolved in ~0.25M HCl, and a slurry of Dowex 50X8, 200-400 mesh resin in the NH_4^+ form is added to the solution. After adsorption of the lanthanides on the resin, the resin is transferred to a column of the same resin. The column is washed first with H_2O and then with 0.5M α-hydroxy-isobutyric acid, pH 3.50. Samarium, neodymium, and cerium are chromatographically separated by elution with 0.5M α-hydroxy-isobutyric acid, pH 3.90. Lanthanum is eluted with 1.0M α-hydroxy-isobutyric acid, pH 4.5. Small fractions are collected and counted for Eu, Pm, and Ce activity to identify the location of the individual fission product lanthanides. Based on prior knowledge of the elution characteristics of the column and specific lanthanides, the fraction containing the major portion of each individual lanthanide is selected.

Final purification of the individual lanthanides is obtained by adjusting the acidity of the collected fraction to 1M in HCl, loading the lanthanide on a column of Dowex 50X8, 100-200 mesh resin in the H^+ form, washing the column with 2M HCl, and eluting with 5M HCl. Each individual lanthanide fraction is evaporated to dryness in preparation for mass spectrometric analysis.

Mass spectrometry - Each of the four lanthanides are analyzed in a different manner. In the case of lanthanum and cerium, the oxide beam is used for analysis because barium is a common and persistant

interference. Analysis of the oxide ions minimizes the barium interference because barium does not readily form a BaO^+ ion in the mass spectrometer. In the case of neodymium and samarium, the metal ion is used for analysis because it gives better intensity, stability, and analytical precision, and is not subject to barium interference.

The lanthanum sample is dissolved in ∿0.01 mL 1M HNO_3, loaded onto a prebaked tantalum center filament, dried, and heated to dull red heat for ∿1 minute to force conversion to the oxide. In the mass spectrometer, the temperature is increased until a stable LaO^+ spectrum is obtained. For the unspiked samples, the 139 to 138 oxide ratio is very large, which limits the accuracy of the 138 measurement.

Cerium is prepared for analysis in a manner similar to lanthanum but the isotopes are measured at two different intensity levels. Initially, the oxide beam of mass 140, 142, and 144 is measured. Then the beam intensity is increased ∿20 fold and the 136 to 144 ratio is measured. Because the atom abundance of mass 144 is less than the atom abundance of mass 142 but greater than mass 136, the measurement of a large ratio (i.e., mass 140 to 136) is not required. This improves the accuracy of the measurement.

Each neodymium and samarium sample is dissolved in ∿0.01 mL 1M HCl, loaded on a prebaked tantalum side filament and evaporated to dryness. A prebaked rhenium center filament serves as the ionizing filament. After insertion into the mass spectrometer, about 30 minutes is required to bring the filament to temperature and for the beam to stabilize.

A-3. Zirconium

Chemical Separation - A weighed aliquot of the dissolved sample solution is added to a weighed aliquot of ^{90}Zr spike and mixed. Zirconium is twice precipitated using NH_4OH. The final precipitate is dissolved in 8M HNO_3, loaded on a Dowex 1X8, 100-200 resin column in the NO_3^- form and zirconium eluted with 8M HNO_3. The zirconium ions are then twice precipitated as the iodate using a thorium carrier. The second precipitate is dissolved in 10M HCl and loaded on a Dowex

1X8, 100-200 mesh resin column in the Cl^- form. Thorium is washed through the column with 10M HCl. Zirconium is eluted with 8M HNO_3, and the eluate is evaporated to dryness prior to the mass spectrometric analysis.

Mass Spectrometry - The double filament analysis technique is used for the analysis of zirconium. The dried zirconium sample is dissolved in ~0.01 mL 1M HCl, loaded on a prebaked Ta side filament, and evaporated to dryness. The center ionizing filament is rhenium. The temperature of the center filament is increased as high as possible without producing a Mo^+ background beam. The temperature of the sample filament is slowly increased until the desired intensity and stability of the zirconium beam is attained.

A-4. Molybdenum

Chemical Separation - For concentration measurement, a weighed aliquot of the dissolved sample solution is added to a weighed aliquot of ^{94}Mo spike, mixed, and evaporated to near dryness. The residue is dissolved in 6M HCl-0.2M HF and extracted into methyl isobutyl ketone which has been pre-equilibrated with 6M HCl-0.2M HF. The organic phase is scrubbed first with 6M HCl-0.2M HF and then with 6M HCl. Molybdenum then is back extracted with H_2O and the aqueous phase is evaporated to dryness. The residue is dissolved in 0.1M HCl, loaded on a Dowex 2X8, 100-200 mesh resin column in the Cl^- form, and the column is washed with 0.1M HCl. Molybdenum is eluted with 1.5M HCl and the eluate is evaporated to dryness.

Mass Spectrometry - The sample is dissolved in ~0.01 mL 1M HCl, loaded on a prebaked rhenium center filament, and evaporated to dryness. During the mass spectrometric analysis, mass 90 must be monitored to determine the absence or presence of zirconium which can interfere in the analysis of molybdenum.

A-5. Ruthenium

Chemical Separation - For concentration measurements, a weighed aliquot of the dissolved sample is added to a weighed aliquot of ^{96}Ru spike, and the mixture adjusted to give an $\sim$ HCl to HNO_3 mole ratio of 5:1 or greater. The mixture is placed in a specially designed distillation flask, fumed with H_2SO_4, allowed to cool, and diluted with H_2O. A slurry of solid sodium bismuthate is added and the ruthenium is distilled as RuO_4. The distillate is collected in chilled HCl which is subsequently evaporated to near dryness in preparation for mass spectrometric analysis.

Mass Spectrometry - The sample solution is transferred to a prebaked rhenium center filament and slowly evaporated to dryness (special care must be taken to avoid excessive heating of the filament). After the filament is inserted into the mass spectrometer, the temperature of the sample filament is slowly increased until desired beam stability is attained. Zirconium and molybdenum must be constantly monitored during the analysis because they can be an interference in the ruthenium spectrum.

DISTRIBUTION RECORD FOR ICP 1050-II

Internal Distribution

1 - Chicago Patent Group
9800 South Cass Avenue
Argonne, Illinois 60439

2 - CA Benson
Idaho Operations Office-ERDA
Idaho Falls, ID 83401

1 - HP Pearson, Supervisor
Technical Information

10 - INEL Technical Library

20 - Authors

37 - Special Internal

External Distribution

270 - LMFBR - Fuel Recycle, Base Technology, TID-4500, R65
UC-79c

Total Copies Printed - 341